MUTAGENESIS STUDIES ON CHARGED RESIDUES IN THE HERG K^+ CHANNEL

by

Yue Wu

A THESIS SUBMITTED IN PARTIAL FULFILLMENT OF

THE REQUIREMENTS FOR THE DEGREE OF

MASTER OF SCIENCE

in

THE FACULTY OF GRADUATE AND POSTDOCTORAL STUDIES

(Pharmacology and Therapeutics)

THE UNIVERSITY OF BRITISH COLUMBIA

(Vancouver)

April 2015

Abstract

The loss-of-function mutations in the human ether-à-go-go–related gene (hERG) K^+ channel serve as one of the primary genetic substrates for congenital long QT syndrome (LQTS), and unlike most Kv channels with fast-activating kinetics, hERG channels have unusually slow activation kinetics. Thus, it is a necessary task to understand mechanisms of hERG gating, especially since the charge-rich S4 segments play such an important role in channel opening in response to membrane potential changes. Despite the structural homology to other Kv channels, how individual S4 charges in hERG are positioned and moved under the influence of membrane voltage changes remains controversial. Therefore, this thesis focuses on the molecular basis of individual charge residues underlying S4 movement. To monitor S4 movement associated with the voltage- and time-dependence accessibility by the sulfhydryl-specific agent MTSET, we mutated a series of S4 charges (K525-K538) to uncharged glutamine (Q) in a mutant in which cysteine replaced the isoleucine at position 521 near the top of S4. We found that K525, R528, and R534 mainly secure the S4 position in the resting state. Our results on the rate of S4 movement suggest that R528, R531, and R537 potentially facilitate the transition of S4 from the closed to the active state. Conversely, neutralization of the bottom lysine K538 significantly accelerates the rate of S4 movement, implying an important constraint on S4 by K538. To further investigate this unique role of K538, we measure the gating charge contributions of K538 and D411 (a potential ion-pairing in S1) with the cut-open vaseline gap technique. Our data show that mutations of both charges to neutral residues (K538Q and D411N) accelerate the time dependence of charge movement while both mutant channels are gated with faster kinetics than control over a physiologically relevant range of depolarizations. This highlights the substantial contribution of both residues to slow hERG gating.

Preface

The work that follows was conducted in the laboratory of Dr. David Fedida and in collaboration with Dr. Ying Dou, Dr. Sam Goodchild, and Robert Vander Velde.

The work in Chapter 3 was stimulated by ideas arising from the following published papers: (i) Ying Dou, Samuel J. Goodchild, Robert Vander Velde, Yue Wu and David Fedida. (2013). " The neutral hydrophobic isoleucine at position I521 in the extracellular S4 domain of hERG contributes to channel gating equilibrium." *Am J Physiol Cell Physiol* 305: C468-C478. (ii) Wang, Zhuren, Dou, Ying, Goodchild, Samuel J, Es-Salah-Lamoureux, Zeineb, Fedida, David (2013). "Components of gating charge movement and S4 voltage-sensor exposure during activation of hERG channels." *The Journal of General Physiology* 141(4): 431–43.

The experiments in Chapter 3 were conducted by Dr. Ying Dou and myself. I prepared DNA template and RNA transcripts, and injected RNA into *Xenopus* oocytes. I also participated in conducting the electrophysiology experiments and in analyzing the data. A manuscript of this study will be submitted for publication.

The data, for gating current recording in Chapter 4, were collected by Dr. Ying Dou and myself. I prepared DNA template and RNA transcripts, and injected RNA into *Xenopus* oocytes. I also participated in conducting the electrophysiology experiments and in analyzing the data.

Table of Contents

List of Tables

List of Figures

List of Symbols and Abbreviations

Arg, R	Arginine
COVG	Cut-open Vaseline gap
G-V	Conductance-voltage relationship
Glu, Q	Glutamine
hERG	The human ether-á-go-go–related gene
HEPES	4-(2-hydroxyethyl)-1-piperazineethanesulfonic acid
I_{Kr}	Rapid delayed rectifier current
k	Slope factor
KC1	Potassium chloride
Kv	Voltage-gated potassium channel
Lys, K	Lysine
LQTS	Long QT syndrome
$MgC1_2$	Magnesium chloride
MTSET	[2-(trimethylammonium)ethyl] methanethiosulfonate
NaC1	Sodium chloride
NaOH	Sodium hydroxide
ND96	Extracellular recording solution
Q	Charge
Q-V	Gating charge-voltage relationship
τ	Time constant
TEVC	Two-electrode voltage clamp
V	Voltage

$V_{1/2}$	Half-activation potential
VSD	Voltage-sensing domain
WT	Wild-type

Acknowledgement

Firstly, I would like to express my gratitude to my supervisor, Dr. David Fedida, who has offered me the necessary guidance and the environment to achieve my research goals. I appreciate his invaluable input in data management, presentation skills, and final revision of the manuscript of this thesis. Also, I would like to thank all of my fellow lab members for providing their support and a friendly environment.

I particularly appreciate Dr. Ying Dou for her well-rounded guidance throughout my research works. Her precious advice and support led me in the right paths that were valuable for my project both theoretically and practically. I would also like to thank Dr. Steve J. Kehl and Dr. Harley Kurata for serving as my committee members with their suggestions and valuable comments. Advice, constructive comments and instructions given by Dr. Donald McAfee, Dr. Zhuren Wang, and Dr. Sam Goodchild have been a great help in my research.

Finally, my heartfelt appreciation goes to my parents whose have supported me mentally and financially throughout my graduate studies.

For my parents

Chapter 1: Introduction

1.1 Overview

There are various types of ion channels expressed in every organism. Ion channels are porous membrane proteins located within the lipid bilayer which are selectively permeable to ions based on a combination of their size and charge. The potassium channels are a diverse family of ion channels through which K^+ preferentially permeates. Voltage-gated potassium (Kv) channels that sense changes in membrane voltage contribute to the repolarizing phase of the action potential and control excitability in muscle tissue and nerve. It has been acknowledged that the human *Ether-a-go-go* Related Gene (hERG) potassium channels (KCNH2 or Kv11.1) encodes I_{Kr}, a member of Kv channel family, and plays a significant role in cardiac potential repolarization and in the termination of cardiac systole (M C Sanguinetti et al. 1995; M C Trudeau et al. 1995). Mutations and blockage of hERG/I_{Kr} channels by medications may induce long QT syndrome type 2 (LQT2) (Michael C Sanguinetti and Tristani-Firouzi 2006). Therefore, understanding the details of hERG's mechanism and regulation is crucial. The aim of this chapter is to review the background with a brief synopsis of the structure and gating of hERG channels. This introduction will offer insight into the focus of this thesis, which mainly investigates the regulation of each charged residue related to voltage sensor movement.

1.2 Background of the hERG channel

The original member of the " ether-à-go-go (eag) " family was discovered in a *Drosophila melanogaster* mutant and named due to leg-shaking behavior observed when the flies were anesthetized with ether (Kaplan and Trout 1969). After a few years, a human homolog of *eag* was first cloned by using low stringency screening of a human hippocampal cDNA with a mouse

homolog of the EAG K^+ channel gene (Warmke and Ganetzky 1994) and it is highly expressed in the heart (Curran et al. 1995). The human *eag-related gene* (h*erg*), or gene KCNH2, shares 47-49% homology with other eag and elk (ether-à-go-go-like) gene located on human chromosome 7 (Warmke and Ganetzky 1994). Subsequently, two studies (M C Sanguinetti et al. 1995; Trudeau et al. 1995) showed that heterologous expression of hERG in *Xenopus* oocytes generated the 'rapid' delayed rectifier current I_{Kr}, which could be blocked by the benzenesulfonamide Class III antiarrhythmic agent, E-4031 or dofetilide (M C Sanguinetti et al. 1995; Trudeau et al. 1995). hERG channels showed a maximum conductance at +10 mV or greater, then hERG currents started to show strong inward rectification due to a rapid voltage-dependent inactivation (M C Sanguinetti et al. 1995; Trudeau et al. 1995). From these results, hERG currents are identified as having slow activation and rapid inactivation at positive potentials while showing rapid recovery from inactivation and slow deactivation at negative potentials (M C Sanguinetti et al. 1995; M C Trudeau et al. 1995). Upon repolarization of the action potential, hERG channels open, resulting in an increase of hERG/I_{Kr} currents during the first half of phase 3 repolarization (Michael C Sanguinetti and Tristani-Firouzi 2006).

These special gating properties of hERG/I_{Kr} currents play an essential role in controlling the balance of membrane potential during the plateau phase of the action potential (Michael C Sanguinetti and Tristani-Firouzi 2006), as suggested by the linkage between inherited or acquired long QT syndrome and gene defects, or drug suppression of I_{kr} (Giudicessi and Ackerman 2012). The functional consequence of LQT2 mutations is a net reduction of I_{Kr} current due to modification of the biophysical properties of hERG channels (Nakajima *et al*., 1998: Sanguinetti et al., 1996) or the prevention of the normal trafficking of the channels to the surface (Furutani et al., 1999; Huang et al., 2001; Ficker et al., 2000). For example, the mutation of a

number of residues in the N-terminal region of hERG channels causes acceleration of deactivation and reduced hERG current during the repolarizing phase of the action potential (Chen et al., 1999), while the mutation R784W in the C terminus causes a depolarizing shift in the activation kinetics (Huang et al. 2001). Drug-induced LQTS is a disorder of cardiac repolarization caused by block of hERG channels, resulting in prolongation of the QT interval and associated with the serious multifocal ventricular arrhythmia, *Torsades de Pointes* (Michael C Sanguinetti and Tristani-Firouzi 2006).

1.3 The structure of hERG channel

Although we do not have a crystal structure of the hERG channel, our assumptions and knowledge about hERG channel structure come from comparisons with the KcsA bacterial K^+ channel (Doyle et al., 1998) and the Kv1.2 X-ray crystal structure (Long, Campbell, and Mackinnon 2005). The hERG channel has a proposed membrane topology based on primary sequences alignment with other Kv channels, which are tetrameric transmembrane proteins with each subunit composed of six transmembrane domains (S1-S6) (Figure.1.1). The independent voltage-sensing domain (VSD) of each subunit consists of S1-S4, with the key S4 containing a series of positively charged residues; and then this VSD is coupled with the pore domain forming S5-S6 (Michael C Sanguinetti and Tristani-Firouzi 2006; Warmke and Ganetzky 1994). This section will look at the outline of the structure and function of the pore domain and VSD, especially the key voltage-sensing region of S4.

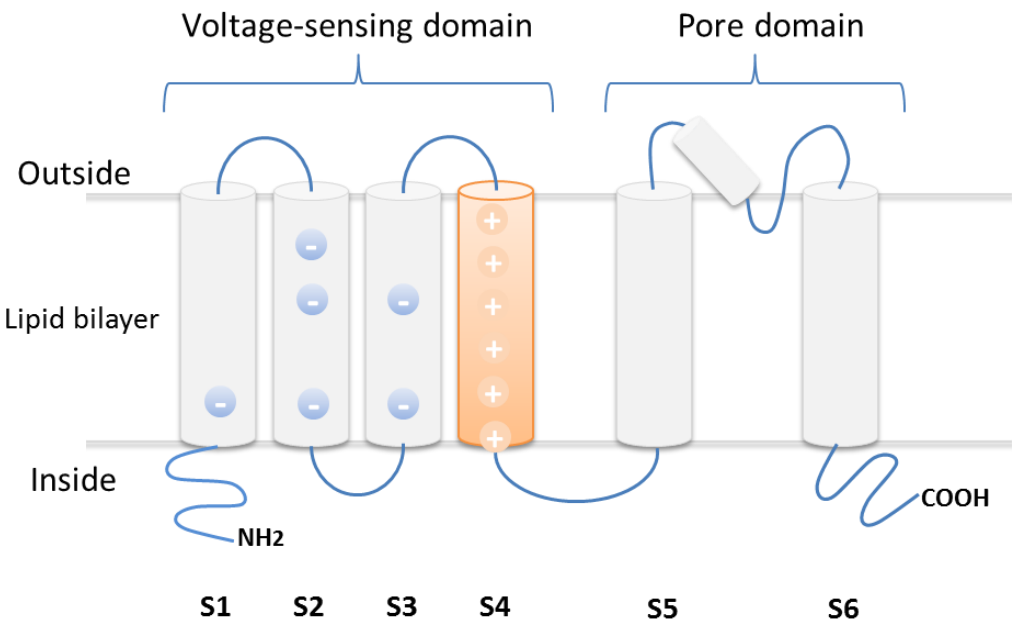

Figure 1.1 Topology of a hERG channel subunit.

A single subunit contains six α-helical transmembrane domains, S1-S6. The S4 domain includes a series of basic amino acids (+) while the S1, S2 and S3 have acidic amino acids (–) which can create salt bridges with particular positively charged residues in S4 during gating.

1.3.1 The voltage-sensing domains

Like other Kv channels, the first four transmembrane segments of each hERG channel subunit form a (VSD). In Kv channels, the fourth transmembrane domains (S4) contain more positively charged residues than other domains. In hERG, the S4 segment sequence (IGLLKTARLLRLVRVARK) with four basic Arg (R) and two Lys (K) residues is mostly separated by two hydrophobic and neutral residues in the α-helical structure (Michael C Sanguinetti and Tristani-Firouzi 2006). It is broadly accepted that charges in the VSD contribute to determining activation kinetics, including transition of the S4 and downstream events in the S4–pore domain interaction. The primary evidence comes from mutations of charged or hydrophobic residues that cause the reduction of the voltage dependence of activation and shift

the voltage range of channel activation (Papazian et al. 1991, 1995). Additional evidences come from the studies in gating current measurement of neutralizing charged residues (Aggarwal and MacKinnon 1996; Seoh et al. 1996). They found that neutralization of three basic residues (R365, R368 and R371) in the S4 of *Shaker* channels remarkably reduced the charge per channel, defining the contribution of those gating charges involved in activation (Aggarwal and MacKinnon 1996; Seoh et al. 1996). On the other hand, K374 in the C-terminal end of S4 had little contribution to the total gating charge per channel (Aggarwal and MacKinnon 1996). For hERG gating, the most critical S4 residue is thought to be the R531 because neutralization of this residue significantly increases the energy perturbation in order to open the channel (Piper et al. 2005; Mei Zhang, Liu, and Tseng 2004). Although we do not have direct structural information about hERG, mutagenesis studies have revealed some particular roles for basic residues in the S4. The past studies mainly suggested that K525 and R531 contribute to the stabilization of the channel in the closed state and in the open state, respectively (Subbiah et al. 2004; Mei Zhang, Liu, and Tseng 2004). Additionally, R534 participates in interactions that stabilize the channel in pre-open closed states (Subbiah et al. 2004; Mei Zhang, Liu, and Tseng 2004). The results of tryptophan scanning of S4 basic residues lead to the conclusion that K525, R528, and K538 are particularly crucial for slow activation of the channel (Subbiah et al. 2005). Importantly, cysteine (Mei Zhang, Liu, and Tseng 2004) and alanine (Piper et al. 2005) scanning mutagenesis studies identified that the outer three charges (K525, R528, and R531) transfer the charges predominantly associated with voltage sensing. Nevertheless, how individual charges contribute to S4 movement itself is not entirely understood.

As proposed in *Shaker* K^+ channels, S4 interactions with the surrounding VSD (S1-S3) seem to have a significant impact on the rate at which S4 segments can traverse the membrane

electrical field (Papazian et al. 1995; Tiwari-woodruff et al. 2000). For *Shaker* K^+ channels, neutralizing K374 causes loss of expression that could be rescued by charge interactions with the neutralized acidic residues (E293Q in S2, D316N in S3), leading to the conclusion that salt bridges between these residues are necessary for protein expression and function (Papazian et al. 1991, 1995). Compared with most Kv channels, the members of the eag family including hERG have three conserved acidic residues (D456, D466 in S2 and D501 in S3), an additional three aspartic acids (D411 in S1, D460 in S2, and D509 in S3), and one extra lysine (K407 in S1). It may be possible that the transient formation of additional charge interactions between these positive and negative residues contribute to the unique gating of hERG channels. hERG D466 in S2 (E293 in *Shaker*) has been suggested to contribute to gating charge transfer (Mei Zhang, Liu, and Tseng 2004) and had potential pairings with K525 and K538R (Cheng et al. 2013). A homologous residue D456 (E283 in *Shaker*) has an intermediate interaction with R534 as the S4 traverses the electric field (Lin and Papazian 2007). In terms of non-conserved acidic residues, early studies indicated that the transient formation of charge interactions between negative and positive charges: D411with K538 in the intracellular side of S4 and D456 with K525 on the extracellular side of S4 was associated with intermediate closed states, implying that both lysines contribute to stabilization of the hERG channel in the resting state (M Zhang et al. 2005). On the other hand, whether or not D411 has cooperative interactions with R531 shows an incompatible result in different studies (Piper et al. 2008; M Zhang et al. 2005). Interestingly, substituted cysteine mutations of atypical acidic residues play a different role in channel opening: both D460C and D509C gave the slow rate of activation with a positive shift of steady-state activation curve, while D411C showed a significantly faster rate of channel activation with a hyperpolarizing shift of activation curve, leading to the conclusion that D411 likely contributes

to stabilize the channel in the closed state (J. Liu et al. 2003). Despite ionic current data on the properties of atypical acidic residues, no studies have investigated their contribution to gating charge movement.

1.3.2 The pore domain

High resolution X-ray structures of bacterial channels (Doyle et al. 1998; Jiang et al. 2002, 2003) showed that the S5, pore helix (P-loop), and S6 transmembrane domains form the pore domain of hERG, and the selectivity filter. Generally, the main gate of the channel is formed by the crossing of four S6 domains, which splay apart to allow ion conductance (Doyle,et al. 1998; Long, Campbell, and Mackinnon 2005). In most Kv channels, the S6 segment has a highly conserved glycine (G) in the middle, which acts as the hinge point during activation gating (Doyle et al. 1998). However, mutations at this position (Gly657) in hERG did not affect channel opening or change the voltage dependence of activation (Hardman et al. 2007). A highly conserved alanine in the middle of S6 marks the narrowest position of the central cavity in most Kv channels. Interestingly, substitution of alanine A653 in hERG with a basic or acidic residue locked the channel in the active state, implying that repulsion of the charges prevents collapse of the bundle crossing (Brown, Sonntag, and Sanguinetti 2008). Most Kv channels have a proline-valine-proline (PVP) motif on the inner side of S6, central to activation gating; however, hERG channels lack this proline hinge and the introduction of a PVP motif into hERG caused a reduction of sensitivity to drugs and prevented channel closure (Michael C Sanguinetti and Tristani-Firouzi 2006). A recent study also found that the introduction of a proline induced a kink in the S6 that prevents the electromechanical coupling of S4 with the pore gate, implying that mutations in the gate can trap the channel gate in the open state (Thouta et al. 2014). The

significant differences in structure between the pore domains of hERG and other Kv channels, and the lack of definitive studies means that a complete understanding of the molecular conformation of the hERG pore domain function remains elusive (Michael C Sanguinetti and Tristani-Firouzi 2006).

1.3.3 The linker between the VSD and the pore domain

According to the crystal structure of the Kv1.2 channel, the S4-S5 linker from the VSD to the pore domain plays a significant role in the electromechanical coupling of hERG channels (Long, Campbell, and Mackinnon 2005; M C Sanguinetti and Xu 1999). In other words, the voltage sensor movement is coupled to channel activation via interaction of the S4-S5 linker with S6 segments (M C Sanguinetti and Xu 1999). In the S4-S5 linker, a single charge-reversing mutation (D540K) caused the re-opening of the channel during membrane hyperpolarization (M C Sanguinetti and Xu 1999). However, a single substitution of R655 with an acidic residue (R655D, R655E) prevents this re-opening in D540K, implying lysine-arginine electrostatic repulsion (D540K-R655) and inward movement of the S4 domain with the D540K mutant (Tristani-Firouzi, Chen, and Sanguinetti 2002). Subsequent work confirmed the contribution of these residues to voltage sensor movement and channel opening because a disulfide bond with cysteine substitution locked the channel in the closed state (Ferrer et al. 2006). Together, the mechanisms by which S4 and S4-S5 linker interactions lead to pore coupling and opening are, are not thoroughly understood and the subject of active investigation.

1.4 The hERG gating properties

Commonly, Kv channels open upon depolarization (activation) and close at resting potentials (deactivation). The K^+ conductance can also be suppressed in activated channels by a different structural process known as inactivation. As opposed to other Kv channels with fast activation and slow inactivation processes, the hERG channel current has a relatively slow activation that precedes the rapid voltage-dependent inactivation process (S. Wang et al. 1997). The time constant of activation of hERG is over 200 ms at 0 mV (Goodchild and Fedida 2013; Michael C Sanguinetti and Tristani-Firouzi 2006), which is much slower than *Shaker* K^+ channels (less than 2 ms) (Zagotta et al. 1994). On the other hand, hERG fast inactivation and recovery from inactivation takes between 1-10 ms, depending on potential, which is much faster than the kinetics of activation and deactivation (S. Wang et al. 1997). These functions are critical to conducting repolarizing currents during the late phase of the cardiac action potential (Michael C Sanguinetti and Tristani-Firouzi 2006) (Fig 1.2).

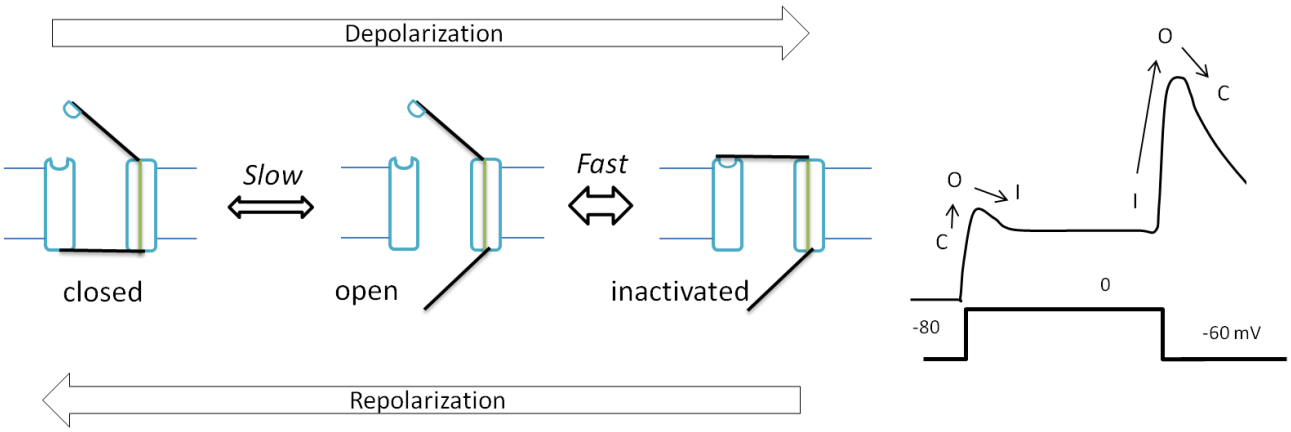

Figure 1.2 Simple diagram of hERG gating.

Left: hERG channels are closed in the resting state. Upon membrane depolarization, hERG channels open slowly (slow activation) and then inactivate rapidly at higher depolarized potentials. These transitions are reversed by membrane repolarization. Right: With a

depolarizing step, hERG channels transit from a closed state (C) to an open state (O) slowly, followed by a rapid inactivation (I) causing little outward currents. With a repolarizing step at -60 mV, hERG channels recover from inactivation faster than deactivation occurs, thereby generating large outward currents (Michael C Sanguinetti and Tristani-Firouzi 2006).

What causes the delay of hERG activation? To answer this question, it is important to examine S4 voltage sensing movement which is recognized as the key determinant of channel activation gating. Several experimental approaches have been developed to offer more insights into the unique mechanisms of hERG gating. First, voltage-clamp fluorometry (VCF) measurement using an attachable fluorometry signal at the outer end of S4 (E519C) enables us to monitor environmental changes near the fluorometry binding site (Smith and Yellen 2002). The subsequent VCF study with E519C:C445V:C449V, which replaced endogenous two cysteines in S1-S2 linker with valines (referring to C-less in this thesis), proved the separation between the fluorometry signal underlying voltage sensor movement and ionic current activation associated with pore-coupling (Es-Salah-Lamoureux et al. 2010). This hyperpolarized shift of the voltage-dependence of the fluorescence signal relative to the conductance-voltage (*G-V*) relation indicated S4 movement can be detected by using VCF measurement with the C-less background (Es-Salah-Lamoureux et al. 2010). Moreover, gating current measurements have been developed to detect the transition of gating charges across the membrane electric field (Goodchild and Fedida 2013; Piper et al. 2003; Z. Wang et al. 2013). Different from macroscopic ionic currents, which measure ion movement via the channel pore from the one side to other side of the membrane, a tiny gating current is recognized as the intramembrane displacement of charged residues in the voltage sensors of the channel, which requires the complete blocking of ionic currents (Bezanilla 2000). The initial gating current measurements of hERG channels noted fast and slow gating components of charge displacement that differed ~100-fold in their kinetics

(Piper et al. 2003). The authors indicate that the slow component carries the majority of the gating charge and results in the slow kinetics of hERG activation, which is ~100-fold slower than *Shaker* gating currents (Piper et al. 2003). In addition, the fast component likely results from rapid transitions during the early stages of the activation pathway between closed states, but its mechanism is still not fully understood (Piper et al. 2003). As shown previously in many gating studies, the hyperpolarizing shift of the voltage-dependence of total gating charge movement (Q_{OFF}-*V*) relative to the *G-V* indicates that voltage sensor movement occurs earlier than channel opening (Bezanilla 2000; Bezanilla et al. 1991). Furthermore, the recent measurements of hERG gating current found that the time constants of charge movement are much faster than those of channel opening, which suggests that S4 movements are not rate-limiting in hERG slow gating, implying that downstream events may have more effect on the delay of pore opening (Goodchild and Fedida 2013; Z. Wang et al. 2013). Thus, the underlying mechanism for the slow activation process still requires further investigation.

Although S4 movement is not rate limiting to channel opening, the time constant of gating charge movement of hERG is still slower than most Kv channels (Goodchild and Fedida 2013; Z. Wang et al. 2013). Several studies have hypothesized potential contributors to slow S4 movement. Firstly, it is possible that fewer basic residues underlie gating charge transfer in S4, which results in a slower motion due to a decreased sensitivity to membrane depolarization (Ahern and Horn 2004; Islas and Sigworth 1999). Additionally, the slow movement of S4 could be induced by additional acidic residues in other VSD regions (S1-S3), by forming salt bridges with S4 basic residues preferentially in closed or pre-open closed states; thus, since hERG has six negative charges (as opposed to three in *Shaker*) in its VSDs, these extra constraints may resist outward movement of the S4 helix (J. Liu et al. 2003; M Zhang et al. 2005). This idea

about the prominent contribution of acidic residues is supported by the single mutation of an acidic residue (D540A or E544A) in the S4-S5 linker, which drastically accelerated the rate of channel activation (M C Sanguinetti and Xu 1999).

The activation time course of hERG current is sigmoidal, which suggests the presence of multiple closed states (C_1-C_2-C_3) prior to the opening transition (C_3-O) (Trudeau et al. 1995; S. Wang et al. 1997) as seen in *Shaker* and other Kv channels (Fedida and Hesketh 2001; Zagotta et al. 1994). The presence of a voltage-independent step between the second and third closed states (C_2-C_3), that becomes rate-limiting at higher depolarized potentials, is proposed in most kinetic models (Goodchild and Fedida 2013; Piper et al. 2003; Subbiah et al. 2004; S. Wang et al. 1997). The reason why the C_2-C_3 transition appears to be a voltage-independent step was based on the strong voltage dependence of the deactivation rate at the final transition to opening, which suggests that the final C_3-O state must be the voltage-dependent (S. Wang et al. 1997). In other words, hERG gating has distinct slow activation with a voltage-insensitive step, which is rate-limiting at depolarized potentials (S. Liu et al. 1996; Trudeau et al. 1995; S. Wang et al. 1997). This phenomenon was experimentally observed with gating current measurement that gating charge movement became saturated at a voltage-independent step in parallel with pore gating (Goodchild and Fedida 2013).

1.5 Substituted cysteine accessibility

The combination technique of cysteine mutagenesis and chemical modification of the substituted-cysteine residues has been widely used to investigate the structure and function of proteins. The sulfhydryl group of cysteine residues is associated with the formation of a disulfide bridge (-SS-) with potential chemical reagents. In the early 1990s, this reactivity has been

utilized as a new approach to introducing a cysteine into the desired position of channel residues which allows a cysteine-binding reagent to bind and modify it (Akabas et al. 1992; Stauffer and Karlin 1994). They created a series of water-soluble chemical reagents based on the methanethiosulfonate (MTS) moiety, named as the substituted cysteine accessibility method (SCAM) (Akabas et al. 1992; Stauffer and Karlin 1994). Since one of MTS reagents, MTSET, has a permanent positive charge which prevents diffusion across lipid membranes, this technique is a valuable tool to measure the time-course and the state dependence of residue modification in electrical recordings (Akabas et al. 1992; Stauffer and Karlin 1994) (Figure 1.5).

Previous studies in our lab have developed an alternative voltage sensor assay by utilizing MTSET modification of a substituted cysteine. Among a series of residues in the S3-S4 regions, it was found that cysteine-substitution of I521 at the outer aspect of S4 caused a substantial hyperpolarizing shift of the G-V relationship following the application of MTSET (Dou et al. 2013; Z. Wang et al. 2013). In addition, I521C residues are only accessible with external MTSET upon membrane depolarization while they have little modification upon hyperpolarization, leading to the conclusion that I521C residues show the state-dependent accessibility to MTSET perfusion (Dou et al. 2013; Z. Wang et al. 2013).

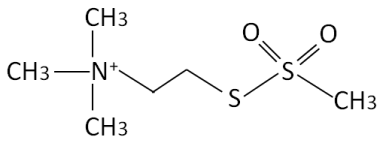

MTSET

Figure 1.3 Molecular structure of MTSET

(2-aminoethyl methanethiosulfonate hydrobromide)

Chapter 2: Methods and Materials

2.1 Molecular biology

The hERG plasmid was subcloned into the pBluescript SK expression vector. All mutations were generated by QuickChange II site-directed mutagenesis methods (Stratagene, La Jolla, CA) confirmed with DNA sequencing by Macrogen (Maryland, USA). For RNA transcription, linearization of cDNA was digested by *NotI* in advance. After purifying linear cDNA, cRNA was synthesized using mMessage mMachine T7 Ultra transcription kit (Ambion, Austin TX). To prevent accidental modification by MTSET, we initially substituted two endogenous cysteines (C445 and C449) with valines on the S1-S2 linker (referred to as C-less in this study); the gating of the C-less mutant showed little difference to the hERG WT channel (Es-Salah-Lamoureux et al. 2010). All currents were recorded in this genetic background (hERG C445V:C449V:I521C).

2.2 *Xenopus* oocyte preparation and expression

All experiments carried out in these studies were approved by the University of British Columbia animal care guidelines, established by the Canadian Council of Animal Care (CCAC). *Xenopus laevis* frogs were anesthetized in $2mg \cdot ml^{-1}$ tricaine methanesulphonate (Sigma-Aldrich, Canada). Stage V-VI oocytes were partially defolliculated by the prepared collagenase solution that contains $2mg \cdot ml^{-1}$ type 1a collagenase (Sigma) in OR2 buffer (in mM: 82.5 NaCl, 2.5 KCl, 1 $MgCl_2$, and 5 HEPES) for about 1h to 1.5h with orbital shaking at room temperature (20 to 22 ℃). Then, oocytes were washed several times with OR2 buffer to remove the collagenase solution. The defolliculated oocytes were initially rocked in an 18 ℃ incubator for approximately 1h in a modified oocyte Ringer solution, containing 500ml Leibovitz's L-15 medium (in mM: 15 HEPES, 0.52 gentamicin, and L-glutamine, adjusted to pH 7.6 with NaOH).

The isolated oocytes were injected using a Drummond microdispensor with 50-100 nl of the cRNA solution containing 50-100ng and incubated for 24-72 h before experimental days. For gating current recordings, oocytes were required to culture at least 3-4 days for high expression. Generally, methods were as in prior studies from this laboratory (Dou et al. 2013; Z. Wang et al. 2013).

2.3 Data acquisition and analysis

2.3.1 Two-electrode voltage clamp recording

Membrane currents were measured from all hERG constructs using the two-electrode voltage clamp (TEVC) technique by using a Warner Instrument OC-725C amplifier (Hamden, CT) and Axon Digidata 1440 A/D converter (Axon Instruments, Foster City, CA), connected to a personal computer running pClamp 10.3 software (Molecular Devices). Oocytes were put in a bath chamber that was constantly perfused with ND96 control solution (in mM : 96 NaCl, 5 KCl, 1$MgCl_2$, 2 $CaCl_2$, and 5 HEPES, adjusted to pH 7.4 with NaOH). The recording microelectrodes were filled with 3 M KCl and had tip resistances of 0.1 to 1.0 MΩ. All experiments were performed at room temperature (20 to 22 ℃). Signals were acquired at a sampling rate of 10 kHz. All parameter values were measured using Clampfit 10.3 software and further analyzed using Graphpad Prism. Statistical comparisons were made using Student's t-test or ANOVA with a Dunnett multiple comparison test. A p-value of 0.05 was considered as significant. All data were measured as mean ± the standard error of the mean (SEM) for the number of oocytes studied for each construct (*n*).

2.3.2 Voltage protocols and calculation

Various voltage protocols were used in the experiments described in this thesis depending on the mutants (e.g., Fig.2). These voltage protocols are noted in relevant figures.

2.3.2.1 Steady-state activation

The steady-state voltage dependence of hERG channel activation can be estimated by the peak conductance-voltage (*G-V*) relationship. To determine the voltage dependence of activation, oocytes were held at -80 mV then depolarized to +60 mV in 10mV increments for 8 s, followed by a 2 s hyperpolarizing pulse to allow the channel to recover from inactivation and close the channel (M C Sanguinetti et al. 1995) (Fig 2.1 A).

Conductance-voltage (*G-V*) relationships were measured from tail currents. Data were fit with a Boltzmann function of the form:

$$y = \frac{1}{1 + \exp\left[\frac{(V_{1/2} - V)}{k}\right]}$$

Where *y* is the conductance normalized with respect to the maximal conductance, $V_{1/2}$ is the half-activation potential, *V* is the test voltage, and *k* is the slope factor.

2.3.2.2 Time course of activation

Like *Shaker* K^+ channels, hERG K^+ channels experience transitions through several closed states before opening, which can be observed from the sigmoidal shape of activation time courses (S. Wang et al. 1997). Time constants of activation can be measured by using an envelope of tail currents measured at hyperpolarized potentials (Wang et al. 1997). Oocytes were held at a

hyperpolarized potential (generally -120 mV) and then depolarized to the individual activating potentials (in the range from -60 to +60 mV depending on the mutants) for increasing pulse durations (Fig 2.1 B). We measured each peak tail current against duration, and fitted the overall envelope with single exponential curves.

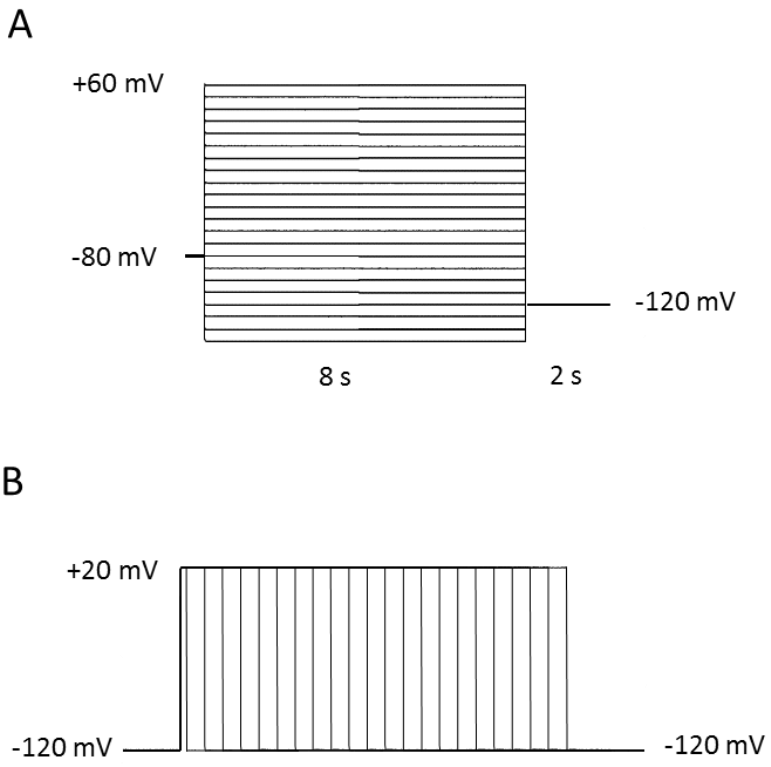

Figure 2.1 Standard voltage-clamp protocols used to characterize the gating of the hERG channel.

(A) Voltage protocol for hERG channel activation. (B) Voltage protocol for the time constant of hERG channel activation (by the envelope of tail currents analysis).

2.3.3 Chemical modification of cysteine

The cysteine-specific binding chemical reagent, MTSET (Toronto Research Chemicals Inc, Ontario), was dissolved in ND96 to 0.1 M. Since the half-time of MTSET activity is ~15 min

(Akabas et al. 1992; Stauffer and Karlin 1994), the MTSET stock solution was diluted to 0.5 or 1 mM, and stored in liquid nitrogen prior to use.

2.3.4 Cut-open Vaseline gap (COVG) recording

Gating current recordings were performed by Cut-open Vaseline gap configuration (CA-1; Dagan Inc) and Dagan CA-1B COVG amplifier (Dagan, Minneapolis) at room temperature (20 to 22℃) (Stefani and Bezanilla, 1998). To diminish the endogenous potassium and chloride conductances from oocytes during COVG recording, oocytes were normally perfused with chloride and potassium-free solutions. The external solution in the top and guard pool consisted of (in mM); 120 tetraethylammonium hydroxide (TEA-OH), 120 methanesulfonic acid (MES), 10 HEPES, 1 CaMES, pH 7.4. The internal solution in the bottom pool was composed of (in mM); 120 TEA-OH, 120 MES, 10 HEPES, pH 7.4. Both solutions contained 20 μM terfenadine to block ionic currents through hERG open channels. To help current access to the oocyte interior through agar bridges, 0.3 % saponin dissolved in internal solution was applied to the bottom chamber for 0.5 to 2 minute. Each agar bridge housed a fine platinum wire and 1 M NaMES. Low-resistance (0.1 to 0.5 MΩ) glass micropipettes were filled with 3M CsCl. To deplete endogenous K^+ ions in the oocytes for hERG gating current recording, the membrane potential was held at 0 mV for 20 to 30 min. Records were acquired at a sampling rate of 25 to 50 kHz with a 5 kHz low-pass filter. P/6 to P/8 protocols from a holding voltage (a range of -80 mV to -110 mV) were used to subtract linear leakages and capacitive currents. Gating current data were analyzed using Clampfit 10.3 software and further analysis was performed within Graphpad Prism using Student's t-test or ANOVA with a Dunnett multiple comparison test.

Chapter 3: Modification of I521C as a probe of function of charged residues

3.1 Introduction

The molecular mechanism underlying the unusually slow activation of hERG channels is not entirely understood. There are two main explanations for this unique gating property. First, the slow movement of the voltage sensor (S4) segments is rate-limiting for channel opening (Piper et al. 2003; Smith and Yellen 2002). Second, extensive salt bridge interactions between negatively charged residues in the S1- S3 transmembrane domain and positively charged residues in S4 might produce structural constraints on voltage sensor movement (J. Liu et al. 2003; Subbiah et al. 2004; M Zhang et al. 2005). Studies using voltage-clamp fluorometry (VCF) on mutant E519:C445V:C449V; however, provided evidence that the S4 segments actually move rapidly (Es-Salah-Lamoureux et al. 2010). In addition, data from MTSET modification and gating current recording revealed that the time constant for activation of S4 is much faster than channel opening (Z. Wang et al. 2013; Goodchild and Fedida 2013). These results indicate that S4 movement precedes pore opening, which is similar to *Shaker* channels (Lidia M. Mannuzzu 1996). Therefore, although the S4 movement of hERG channels is still slower than *Shaker* channels (S. Wang et al. 1997; Zagotta et al. 1994), it is not rate-limiting for pore gating.

Voltage-gated Kv channels have a distinct distribution of positive charges (lysine or arginine residues) in S4 segments that sense electric field changes in response to membrane depolarization (Papazian et al. 1991; Seoh et al. 1996). One of the alignment models (Lee, Banerjee, and MacKinnon 2009) has proposed that hERG contains 5 positively charged residues (K525, R528, R531, R534, R537), followed by an extra lysine (K538) adjacent to the bottom of S4 (Fig. 3.1). Because of poor conservation at the sequence level between hERG and *Shaker* channels, it is hard to determine the correct alignment and the exact border of transmembrane

segments in hERG. However, it has been widely accepted that hERG channels have the particular lysine side chain at both extremes of the S4 segment instead of arginine as *Shaker* (Vandenberg et al. 2012). For *Shaker* channels, neutralizing mutations revealed that the first four basic residues on S4 (R362, R365, R368, and R371) have a dominant contribution to gating charge relative to channel activation and K380 likely has a minor contribution (Aggarwal and MacKinnon 1996; Seoh et al. 1996). For hERG channels, it has been suggested that the outer three charges (K525, R528, and R531) contribute to gating charge transfer during activation (Mei Zhang, Liu, and Tseng 2004). Moreover, charge neutralization studies showed the outer (K525) and inner lysine (K538) are involved in stabilizing the resting state whereas the neutralization of the middle arginine on S4 (R531) has the opposite effect (Cheng et al. 2013; Subbiah et al. 2004). For K525, Subbiah and colleagues indicated that the addition of the positively charged MTSET to K525C did not restore hERG WT gating properties (Subbiah et al. 2004). Subsequently, replacing K525 with another basic amino acid (K525R) destabilized the closed state as predicted from studies in *Shaker* (Cheng et al. 2013; Tao et al. 2010). Meanwhile, neutralizing K538 causes a hyperpolarized *G-V* and a faster rate of channel activation than hERG WT channels, while K538R induced a depolarized *G-V* and a slower activation kinetic (Cheng et al. 2013; Subbiah et al. 2004). In addition, in an alanine-scanning study, mutation of K538 to alanine caused perturbation of activation without altering associated gating charge movement, suggesting this residue might be involved in coupling voltage sensor movement to channel opening (Piper et al. 2005). Plus, the study of gating measurements in *Shaker* channels led to the conclusion that lysine substitution at the outermost arginine led to a greater stabilization of the closed state than arginine (Tao et al. 2010). Together, the presence of the lysine side chain may be more important to restore the hERG WT gating properties (Vandenberg et al. 2012).

To date, various studies have suggested that the size or structural orientation of these positive residues and the electrostatic interaction between transmembrane domains may affect the stabilization of channel activation and deactivation (Subbiah et al. 2004; M Zhang et al. 2005; Mei Zhang, Liu, and Tseng 2004). However, these effects of charged residues in regulation of S4 movement itself are still unclear. The previous alanine-scanning study on S4 sequence (G514-Y545) depicted a spiral pattern of position of the charge-perturbing mutations on S4 homology model (Piper et al. 2005). The largest perturbation in charge movement only happened in R531A among a series of basic residues (Piper et al. 2005). At the same time, the authors found that neutralization of the top two residues to alanine (K525A and R528A) results in no functional channel expression with gating current measurement (Piper et al. 2005).

It is known that changing the electric field around S4 or an outward movement of S4 in response to membrane depolarization can cause charge movement (Yang, George, and Horn 1996). Several studies proved an outward S4 motion by using membrane-impermeable and permanently charged chemical reagents, MTSET (Akabas et al. 1992; Larsson et al. 1996; Yang, George, and Horn 1996). A series of cysteine-substituted residues on S4 have demonstrated different patterns of state-dependent accessibility to MTSET (Yang, George, and Horn 1996). One potential experiment is to test whether intracellular or extracellular MTSET can access a given residue and how that accessibility changes in an open or closed state of the channel associated with S4 segments (Rocheleau and Kobertz 2008; Mei Zhang, Liu, and Tseng 2004). Recently, we found that an engineered cysteine on the position isoleucine 521 (I521C) on the outermost of S4 segments of hERG could form covalent disulfide bonds with MTSET, in a state-dependent manner (Dou et al. 2013; Z. Wang et al. 2013). I521C was buried in the membrane at the resting potential whereas it was exposed to external MTSET upon depolarization, indicating

that the modification on I521C could reflect the S4 outward translational movement (Dou et al. 2013; Z. Wang et al. 2013) (Fig 3.1 A). This state-dependent modification of I521C by MTSET enables us to monitor S4 movement directly.

Our results suggest that R528, R537, and R531 facilitate the S4 transition from the resting state to the active state. R528 and R537 differently affect the kinetics of S4 movement whereas they have a similar impact on the voltage-dependence of S4 movement. Among charge mutations, R531Q has more impact on the speed of S4 movement itself whereas R528Q causes a slower rate of channel opening over S4 movement. On the other hand, the loss-of-charge on K538 causes a significant acceleration of S4 kinetics with a small effect on pore-opening, which suggests that K538 favors S4 movement from the resting state.

3.2 Influence of charge neutralization on channel activation

To assess the effects of charge mutations on the steady-state channel activation, we mutated each positive charge along S4 of hERG (K525, R528, R531, R534, R537, and K538) to glutamine (with uncharged polar side chains) within the I521C background. Note that the indication of I521C: C-less (see Chapter 2) is omitted for simplicity in this chapter. Representative currents from I521C: C-less (control) and individual mutants are shown in Figure 3.2 A. The conductance-voltage (*G-V*) curves are derived from the peak tail currents against the preceding voltages, fitted with the Boltzmann function (Fig. 3.2 B). To ensure full opening of hERG channels, we apply 8 s long depolarizing pulses, followed by 2 s hyperpolarizing potentials to acquire tail currents. The $V_{1/2}$ of *G-V* curve of control was -28.2 ± 1.2 mV (Table 1).

Most glutamine mutants of S4 affected the steady-state activation, with the exception that R537Q ($V_{1/2}$ = -23.9 ± 2.3) caused only a minor hyperpolarized-shift of the *G-V* curve. Compared

to the control, K525Q, R528Q, R534Q, and K538Q displayed inward currents at the hyperpolarized steps, indicating that these mutations facilitated opening of the channels. The K525Q mutation had the largest impact on steady-state activation ($V_{1/2}$ = -100.0 ± 2.3, n=7), showing an approximate 50% opening probability at -150 mV. On the other hand, R531Q showed a substantial right-shift of the *G-V* curve (Fig. 3.2 B, ■).

3.3 Voltage dependence of MTSET modification of I521C represents voltage dependence of voltage sensor movement

Our previous data showed that the substituted cysteine at I521 residue can be modified by MTSET only in the active state (Dou et al. 2013; Z. Wang et al. 2013). In other words, we can use this residue to identify the accessibility of S4 or the rate of S4 movement. To define the accessibility of MTSET to I521C in the various states, the following voltage-step protocols were used. The magnitude of current was typically recorded for 8 s at 40 mV and then an 8 s hyperpolarizing step was applied to allow the channel to fully deactivate before (gray trace in Fig. 3.3 A) and after (black trace, Fig. 3.3 A) MTSET exposure. At more positive potentials, channels with I521C were exposed to external MTSET for 10 min, followed by a 10 min wash step to remove any noncovalent binding of MTSET (Fig. 3.3 A). The MTSET accessibility at various potentials was evaluated with the extent of irreversible inhibition of channel closing. Generally, the minor modification was observed at hyperpolarized potentials while the significant modification was detected at depolarized potentials (Fig. 3.3 B). As indicated by the triangle symbols, the current amplitudes (*I*) at both peak and end of the repolarization pulse were measured. The change of the ratio of *I* end per *I* peak before and after MTSET application was measured and normalized to the maximal value at a series of holding potentials (ranging

from -120 mV to +60 mV) (Fig 3.3 C). To minimize differences between batches of oocytes, we tried to make a series of recordings at various potentials on the same batch of oocytes. The voltage-dependence of MTSET modification at I521C is well-fitted with a Boltzmann function. Compared with the *G-V* curve of I521C, the midpoint position of the modification curve showed a ~20 mV hyperpolarized-shift ($V_{1/2}$ = -51.4 mV), suggesting that the voltage-dependent MTSET modification on I521C represents the voltage dependence of S4 movement (Fig. 3.3 C). Note that the hERG channel with I521C background is considered as the control in this study.

3.4 Voltage-dependent accessibility of charge mutations on S4

To further examine the importance of the gating charges on the voltage-dependent exposure of S4, we used the method described above. Mutant hERG channels with I521C exposed to extracellular MTSET showed left-shifted GV relationships that caused negative currents upon membrane hyperpolarization. In these experiments, oocytes did not tolerate negative holding potentials less than -120 mV for long periods (-110 mV for R531Q). These effects for each mutant are described in Fig. 3.4 A: K525Q, R528Q, R531Q, R534Q, R537Q, and K538Q. We found two main patterns of voltage-dependent MTSET reactivity depending on the location of the positive residue (see Table 3.1, the lane for S4 movement). R528Q, R534Q, and K538Q modification-voltage relationships showed a substantial negative shift, whereas R531Q displayed a significant positive shift (Fig. 3.4 B). At one extreme, the R531Q modification curve showed a very shallow slope and right-shift ($V_{1/2}$ = -19.3 mV, k =25.0) compared to the control, I521C ($V_{1/2}$ = -51.4 mV, k =19.0). At the other extreme, K525Q mutations remain the largest inward currents even after a 8 s deactivation pulse at -140 mV such that the currents for the K525Q mutant could not be fitted to a Boltzmann relation (Fig. 3.4 B yellow squares). Each mutation

showed different open probabilities after 8 s deactivation at -140 mV before MTSET application (Fig. 3.4 B, as shown in colored bars). Here, we measured the delta ratio of *I* end per *I* peak (Δ *I* end / *I* peak) during the hyperpolarized pulse before and after MTSET where membranes were held at various potentials during MTSET exposure (Fig. 3.4 C). The value of Δ *I* end / *I* peak of K525Q, R528Q, and R534Q increased almost twice as much as control at -120 mV, suggesting that I521C is extruded in these mutants and already accessible to external MTSET. In order to examine the degree of S4 extrusion, we further compared the magnitude of Δ *I* end / *I* peak at -120 mV with the maximum Δ *I* end / *I* peak of MTSET modification (Fig. 3.4 D). Our data indicated that K525Q was approximate 64 % extruded while R528Q and R534Q displayed 31% and 33%, extrusion, respectively. The activation of S4 with K525Q showed the largest value, indicating that K525 is required to stabilize S4 in the closed state. On the other hand, R531Q, R537Q, and K538Q showed a minor modification at -120 mV as well as control, indicating that the position I521C in these mutants is completely buried in the membrane (Fig. 3.4 D). It is possible that K525, R528, and R534 are much more important for stabilizing the channel in the resting state than R531, R537 and K538 at -120 mV. More remarkably, only R531Q showed the property of having a substantial right-shifted in the MTSET modification curve and a shallow slope (Fig. 3.4 B, ■). This suggests that R531 confers sensitivity to voltage and efficiently stabilizes the active state of S4.

3.5 Effects of charge mutations on kinetics of activation

The kinetics of activation are measured using an envelope of tails protocol at 0 mV and 60 mV and representative currents recorded from control and each mutant are indicated in Fig. 3.5. The incremental amplitude of peak tail current at increased durations of the depolarizing pulses can

be fitted with a single exponential function. Time constants (τ) of activation at 0 and 60 mV for all mutations are summarized in Fig.3.5 B. Compared with control (176 ± 26 ms), K525Q (93 ± 21), R534Q (95 ± 12), and K538Q (53 ± 7) channels at 0 mV showed a faster rate of activation while R528Q (494 ± 25), R531Q (247 ± 9), and R537Q (364 ± 17) had a slower rate of activation (see Table 2).

3.6 Effects of charge mutations on the time course of S4 movement

To track the time-constant of voltage sensor movement, we used a protocol with various duration pulses as described previously (Rocheleau and Kobertz 2008; Z. Wang et al. 2013). Oocytes, which were held at -120 mV to prevent early I521C modification by MTSET, were depolarized for 0.05 s short test pulses per 0.5 s cycle, followed by pulses of various fixed durations that kept them depolarized for 10% of the total protocol duration. Since it was only the 10% time spent depolarized that allowed exposure of I521C to MTSET, we called these "10% duty cycle protocols" (Fig. 3.6 A). Applying a short pulse (0.05 s / 0.5 s) was a prerequisite to subtract nonspecific effects of MTSET, which could be washed off. To sustain the constant reactivity of MTSET reagents, which have a short half-life (Akabas et al. 1992; Stauffer and Karlin 1994), we applied freshly prepared MTSET during the whole process for those continuous protocol steps. On the application of MTSET, the decay of currents (which eventually reached a plateau) was well-fitted with a single exponential function to represent the complete modification of I521C. There are three factors that can affect the modification rates of I521C. First, the concentration of MTSET needs to be in excess and was kept constant by adjusting the flow rate of MTSET solution to 2 ml per minute. Second, the local conformational changes around I521C for each mutant itself upon repolarization should be the same. Third, the accessibility of the introduced

cysteines on I521C exposed to MTSET would affect the rate of modification. Taking I521C as an example (Fig. 3.6 B), the modification rate at shorter pulse durations (10/100ms) became slower while longer pulse durations (0.4 /4 s) induced a faster modification rate, which could be experimentally distinguished (Fig. 3.6 C). We could see the modification rate became independent from pulse duration when we applied the longer pulse duration (e.g., 0.1- 0.4 s) to allow S4 to reach equilibrium. In other words, 0.4 s pulses can give the maximum modification rate, while the 10-ms pulse is too short to give enough time for S4 movement (Z. Wang et al. 2013).

By utilizing this particular pulse protocol, we observe different patterns of MTSET modification rate for neutralized S4 positive residues (Fig 3.6 D and Table 2). According to our MTSET modification-voltage curves (Fig 3.4 B), control and R531Q reach maximum activation at 0 mV and 60 mV, respectively. At one extreme, the low open probability of R531Q at 0 mV (Fig. 3.4 B, filled squares) where S4 segments were not fully in the active state, suggests a low binding probability to external MTSET at I521C. In addition, this mutant did not tolerate holding potentials of -120 mV so that we modified its protocol by holding at -110 mV and pulsing to +60 mV.

As indicated previously (Z. Wang et al. 2013), we observed more rapid S4 movement at 60 mV than 0 mV for control (Table 2). At +60 mV, the rate of modification at R531Q (227.8 ± 87.1 ms, $P< 0.05$) was ~16-fold slower than the control (8.5 ± 1.1 ms). Since the S4 movement at 0 mV for control is ~4-fold slower than that value of R531Q at +60 mV, the idea of even slower S4 movement of R531Q at 0 mV seems likely, suggesting that R531Q significantly slows the S4 transition from the resting to the active state. For R528Q, although it was already activated at -120 mV and became maximally activated at -20 mV, we observed slow S4

movement even at 0 mV (100.0 ± 20.1 ms, P< 0.05). For both R534Q and R537Q, we observed voltage-dependent modification at 0 mV that was similar to control; however, the open probability of R537Q at -120 mV was similar to control but not R534Q. Thus, R537Q slows S4 movement (τ = 214.2 ± 80.5 ms) from the resting to the active states whereas it seems likely that pre-existing activation of S4 in R534Q at -120 mV causes a shorter time constant for S4 to reach equilibrium (22.7 ± 8.5 ms) compared to control (57.0 ± 13.7 ms, P < 0.05). At the other extreme, K538Q had the fastest time constant of S4 movement (16.2 ± 9.2 ms, red squares, P < 0.05). Since it is important to compare the same active potential where the voltage-dependence of S4 modification just reaches its maximum value, we further assessed the rate of S4 movement at -30 mV for K538Q *versus* at 0 mV for control. Although the time constant of activation at -30 mV for K538Q (195 ± 26 ms) is similar to that for control at 0 mV (176 ± 26 ms), the S4 movement for K538Q (26.5 ± 9.7 ms) is almost twice as fast as control (57.0 ± 13.7 ms, P< 0.05). Because I521C with K525Q was already fully accessible to extracellular MTSET when the channel was hyperpolarized at -120 mV, we could not apply the 10 % duty cycle protocols to measure the rate of S4 movement for K525Q. With the single mutant K525 (without I521C), we observed a lower open probability at -120 mV, presumably suggesting an additive role of I521C and K525Q on the stability of closed channels (Fig A.1).

Our measurements of the kinetics of voltage sensor movement indicate that R528, R537, and R531 facilitate the transition of S4 from the resting to the active states because of the slow S4 motion associated with neutralization on these basic residues. On the other hand, the time constant of S4 movement for K538Q is 2-fold faster than control, indicating that the neutralized K538 residue causes the rapid S4 movement but does not affect the kinetics of channel opening.

To summarize our findings for the effects of mutations on S4 movement, we measured the ratio of the kinetics of S4 movement and pore opening (Table 2, right column). For control this is 0.32 at 0 mV and 0.16 at 60 mV, respectively. R528Q slowed S4 kinetics and channel opening, but the ratio of 0.20 implies that R528 may have indirect effects on the coupling of S4 movement to pore opening. R531Q markedly prolonged the τ of S4 movement and channel opening; however, the ratio of them significantly increased (0.92), suggesting that neutralization of R531 mainly slows S4 movement rather than affecting the relationship between S4 movement and activation gate opening. A similar situation was observed in R537Q, but to a lesser extent than R531Q. K538Q showed the same rate of channel opening, but it had much faster S4 movement compared with control (0.14), implying that K538 may exert an intrinsic and unique constraint on S4 movement and that rate-limiting steps downstream of S4 movement, that control channel opening, are independent of this residue.

3.7 Discussion

This study provides a valuable insight into hERG voltage sensor movement by defining the pattern of MTSET modification with cysteine-substituted I521 for each charge mutation. Our findings indicate that residues K525, R528, R534, and K538 play a role in stabilizing S4 in the resting state. In terms of time constant of S4 movement, R528, R531 and R537 facilitate the transition of S4 segments from the resting to the active state. Of the positively charged mutations, R531 residues show the largest impact on the kinetics of S4 movement. Remarkably, our data find that neutralizing K538 only influences the rate of S4 movement, but not channel opening, implying that K538 may be a key constraint on S4 voltage sensor movement. These

results confirm the idea that each S4 basic residue makes different contributions to the regulation of voltage sensor movement.

3.7.1 Directly tracking the movement of the voltage sensor

The movement of the voltage-sensing mechanism in voltage-gated potassium channels has been widely studied in *Shaker* channels (Bezanilla 2000). Generally, the displacement of a series of positively charged residues (lysine or arginine) in S4 through the membrane electric field causes the opening of the pore gate and subsequent flux of K^+ ions. Many studies have investigated the voltage sensor operation in hERG channels by using different methodological approaches such as the VCF technique (Es-Salah-Lamoureux et al. 2010; Van Slyke et al. 2010; Smith and Yellen 2002) and gating current measurement (Goodchild and Fedida 2013; Piper et al. 2003, 2005; Z. Wang et al. 2013). In recent studies with the VCF technique, the authors observed environmental changes in the S3-S4 linker upon either depolarization or repolarization relative to hERG channel gating (Es-Salah-Lamoureux et al. 2010; Smith and Yellen 2002); nevertheless, it is still challenging to confirm exact reorganizations of channel conformation from VCF signals. Meantime, gating currents of hERG channel have been recorded from both mammalian cells and oocytes, but some mutations in S4 showed low efficiency of expression for gating current measurement (Piper et al. 2005; Z. Wang et al. 2013). Our previous studies revealed that I521C binds MTSET in a state-dependent manner (Dou et al. 2013). Consistent with data from gating currents and fluorescence recordings (Es-Salah-Lamoureux et al. 2010; Goodchild and Fedida 2013; Z. Wang et al. 2013), MTSET modification of I521C causes a hyperpolarizing shift in the voltage dependence of S4 curves compared with *G-V* curves, indicating that S4 movement precedes pore opening (Fig. 3.4) (Dou et al. 2013; Z. Wang et al. 2013). By utilizing a protocol

first used in KCNQ1 (Rocheleau and Kobertz 2008), the modification rate of I521C against the function of pulse duration enabled us to track the time constant of S4 movement (Z. Wang et al. 2013). Unlike gating current measurements, which tracks the net charge movement, the I521C method can directly track the conformational transition of S4 segments. Gating charge recording in wild-type (WT) hERG channels showed a τ of 88 ms at 0 mV which is ~ 3-fold faster than channel opening (the ratio to the τ of activation is ~ 0.33) (Goodchild and Fedida 2013). The τ of S4 movement for I521C hERG channels at 0 mV is 57 ms and its ratio to the τ of activation is 0.32 (Table 2), which is consistent with the published gating current measurement. These results indicate that MTSET-modified I521C used in this study is a reliable way to directly track S4 voltage sensor movement.

3.7.2 How do S4 charge mutations impact the voltage dependence of S4 movement?

In previous studies, neutral (W, Q, C, A) and reverse-charge (D and E) mutations at two lysines (K525 and K538) indicated a negative shift in the voltage-dependence of activation (Cheng et al. 2013; Piper et al. 2005; Subbiah et al. 2004, 2005; M Zhang et al. 2005). Furthermore, gating current measurement of the K538A mutation showed a ~ 20 mV negative shift compared with WT (-21.9 mV), but there is no gating current recorded from K525A due to low expression (Piper et al. 2005).

Our results confirm that neutralization of two lysines (K525 and K538) markedly affects the voltage dependence of activation. Additionally, we find the active state probability of K525Q was almost the maximum at -120 mV, which supports the idea that this lysine stabilizes S4 in the resting state. Compared with our measurements of K525Q without the I521C background ($V_{1/2}$ = -100.5 ± 0.7) ($V_{1/2}$ = -84.9 ± 1.4 at Subbiah et al. 2004), we observed a large inward current even

at -150 mV, indicating that this adduct at position 521 near K525 may affect closed state channel stabilization (Fig A.1). We see the influence by I521C on R528Q and R534Q which have a hyperpolarized shift in the steady-state activation compared with single mutation of these residues (Subbiah et al. 2004). The S4 probability of R528Q and R534Q at -120 mV is relatively high, and the voltage dependence of S4 for these residues showed a negative shift. Interestingly, neutralization of K538 (K538Q) caused a significant hyperpolarization of MTSET modification-voltage relationships (see Fig 3.4 B), but the charge-conserving mutation on K538 (K538R) showed a similar value to the control, indicating the importance of the positive charge at position 538 (see Appendix, Fig A.2). In terms of voltage-dependence of S4 movement, K525, R528, R534 and K538 are thought to favor salt bridge formation in the resting or the later closed states.

Similar to the steady-state activation relationship reported previously (Piper et al. 2005; Subbiah et al. 2004), our data on R531Q displayed the largest positive-shift of the voltage dependence of S4 movement. Conversely, R371Q in *Shaker* (suggested as an equivalent mutation to R531Q) showed a negative shift in channel activation (Aggarwal and MacKinnon 1996; Seoh et al. 1996), implying the different contribution of hERG R531 during channel activation. Our direct measurements of S4 charge movement imply that R531 residues may favor salt-bridge formation in the active state.

3.7.3 How do charge mutations affect the time constant of S4 movement and channel opening?

To further interrogate the relationship between S4 movement and opening of hERG channels, we examined the kinetics of the processes by utilizing MTSET modification on I521C (Z. Wang et al. 2013). Here, we directly assess the kinetics of S4 movement based on the our measurement

on MTSET modification-voltage curves which provide the information about the maximum modification value with each mutations (0, 60 and -30 mV only for K538Q). First of all, our measurements with I521C confirm that R528Q, R531Q, and R537Q slow the channel activation while K525Q, R534Q, and K538Q accelerate rates of channel opening, which is consistent with previous studies (Cheng et al. 2013; Subbiah et al. 2004).

In general, the left-shifted *G-V* of these mutations (K525Q, R534Q, and K538Q) was associated with a faster rate of activation. Interestingly, R528Q showed a negative shifted *G-V* but a slower rate of activation. A previous study of the charge-reversal mutation R528D also displayed ~20-fold slower activation (but the steady-state *G-V* was the same as control) and ~40-fold slower deactivation (M Zhang et al. 2005). We confirmed in this study that charge-neutralizing with R528 induced either destabilization of closed states or stabilization of the open states, resulting in slower S4 transition. One possible explanation is that the upward movement or rotation of position R528 upon depolarization normally allows interaction with negative charges in other regions of the VSD. Disruption of those interactions may cause destabilization of open and closed conformations of the channel. However, which negative charge(s) contribute to the interactions with R528 to restrict or facilitate S4 movement requires further study.

To compare the S4 movement of each mutation, we used a depolarized test potential, which is equivalent to the value where S4 segments with mutations just reach their maximal probability of being in the active state (0 mV for most mutations, -30 mV for K538Q, Fig.3.4 B). To directly track the time constants of S4 movement, it is crucial to prevent pre-exposure of I521C residue to MTSET. Since neutralizing K525 causes destabilization of the closed state, I521C with this mutation has been already exposed to external MTSET. Still, the impact of other neutralizing charged residues on the voltage sensor movement can be detected by MTSET modification of

I521C. At one extreme, R531 shows the largest impact on S4 movement (Table 2), which is consistent with gating current measurement from alanine scanning mutagenesis (Piper et al. 2005). The authors show that R531A causes the largest perturbation in ΔG so that R531 in hERG channels may play a critical role in voltage sensor movement (Piper et al. 2005). Although their data with analysis of perturbed activation indicated that R528, R534, and R537 were less important to hERG gating, we found R528 and R537 facilitated the transition of S4 from the resting to activated states. This may be because their study focuses on the different energetics of the two states while ours addresses the time constant of S4 movement.

Previous studies in *Shaker* revealed that the first 4 basic residues make the largest contribution to gating charge during channel activation and the individual positively charged residues contribute to activation differently (Aggarwal and MacKinnon 1996; Seoh et al. 1996). Compared to *Shaker* channels, the distribution of charged residues of hERG channel is different in two aspects. First, the S4 segment of hERG has one less gating charge, while it is still suggested that the outer 3 residues (K525, R528, and R531) transfer most of the gating charge upon depolarization (Mei Zhang, Liu, and Tseng 2004). Our data show that R531 is a core determinant of the voltage dependence and kinetics of S4 movement, which is similar to the gating probabilities of R368 (the third charged residue from the top of S4 in *Shaker*; D. M. Papazian et al. 1991; Santacruz-toloza, Bezanilla, and Papazian 1994). Unfortunately, due to the poor conservation of alignment between *Shaker* and hERG, it is hard to directly compare hERG with *Shaker*. Second, hERG has three acidic residues (D411, D460, and D509) in addition to the widely conserved acidic residues in other Kv channels (D456, D466, and D501). It has been suggested that the relatively slower S4 movement of hERG than *Shaker* channels could be influenced by additional electrostatic bonds between those extra acidic residues (J. Liu et al.

2003; M Zhang et al. 2005). Our data on the rate of MTSET modification show that R528, R534 and K538 play important roles in stabilizing S4 in the closed state, implying that the intrinsic salt bridges of these residues with surrounding acidic residues on other VSD may contribute to slowing S4 movement. Although other positive residues are evenly distributed every three, hERG has two continuous positive residues (R537 and K538) at the innermost edge of S4. In this study, the MTSET modification-voltage curves indicate that these two consecutive basic residues affect S4 movement differently. R537 contributes to the stabilization of the active state whereas K538 residues contribute to the stabilization of the resting state. K374 at the bottom of S4 in *Shaker* is suggested to stabilize the channel in the open state (Pless et al. 2011), suggesting that hERG K538 may not be the analogous residue to *Shaker* K347. Interestingly, K538Q showed the largest changes in the kinetics of S4 movement but did not affect the channel activation. A recent study proposed that the charge-conserving mutation K538R had a slower rate of channel activation and a depolarized G-V curve compared with the hERG WT channel (Cheng et al. 2013). This suggests that the loss-of-charge on K538 may disrupt channel closing whereas the lysine-to-arginine mutation on K538 can even facilitate the closing of the channel. By using MTSET modification on I521C, we further tested the voltage- and time-dependence of MTSET modification of K538R (Fig A.2). The slower rate of S4 movement of K538R (145 ms *vs.* 54 ms in control) indicated that the lysine-to-arginine mutation may favor stabilizing the S4 in the closed state. Compared with K538R, which slows both S4 movement and pore-coupling, the time constant of the S4 transition of K538R is only 3-fold slower, while the time constant of channel activation is 10-fold slower than control. These differences imply that R531Q mainly slows the kinetics of S4, whereas K538R significantly delays both S4 and pore-coupling.

Our experiments were conducted to determine not only the voltage-dependence of S4 movement but also the time-dependence of the S4 movement of charge mutations. A definite pattern of state-dependent modification consistent with S4 movement shows that the top lysine K525, R528, R534 and the last lysine K538 stabilize the closed state or destabilize activated states. Meanwhile, slow S4 movement with neutralizing R528, R531, and R537 indicate that they intrinsically facilitate the S4 transition from the resting to activate states. To understand the effect of charge mutations on the coupling between S4 and pore opening, we calculated the ratio between them, suggesting that R528 may affect both voltage sensor and pore-opening. Two continuous basic amino acids (R537 and K538) on the intracellular side of S4 voltage sensor have distinct differences on their voltage-dependence and kinetics of S4 movement. While R537Q slows the rate of channel activation and S4 movement, K538Q significantly accelerates S4 movement with little influence on channel activation. Among charge mutations, only K538Q facilitates S4 movement without altering the rate of channel opening. Meanwhile, the supplemental studies on K538R demonstrate not only slow opening but also delay of S4 movement, which suggests that arginine substitution of this residue may affect both S4 and pore coupling. Furthermore, as the crystal structure reveals (Long, Campbell, and Mackinnon 2005), R537 and K538 should have different charged surfaces of electrostatic interaction with surrounding voltage-sensor domains (S1-S3) that may affect the rate of S4 motion (Fig 3.1 B).

3.8 Figures and Tables

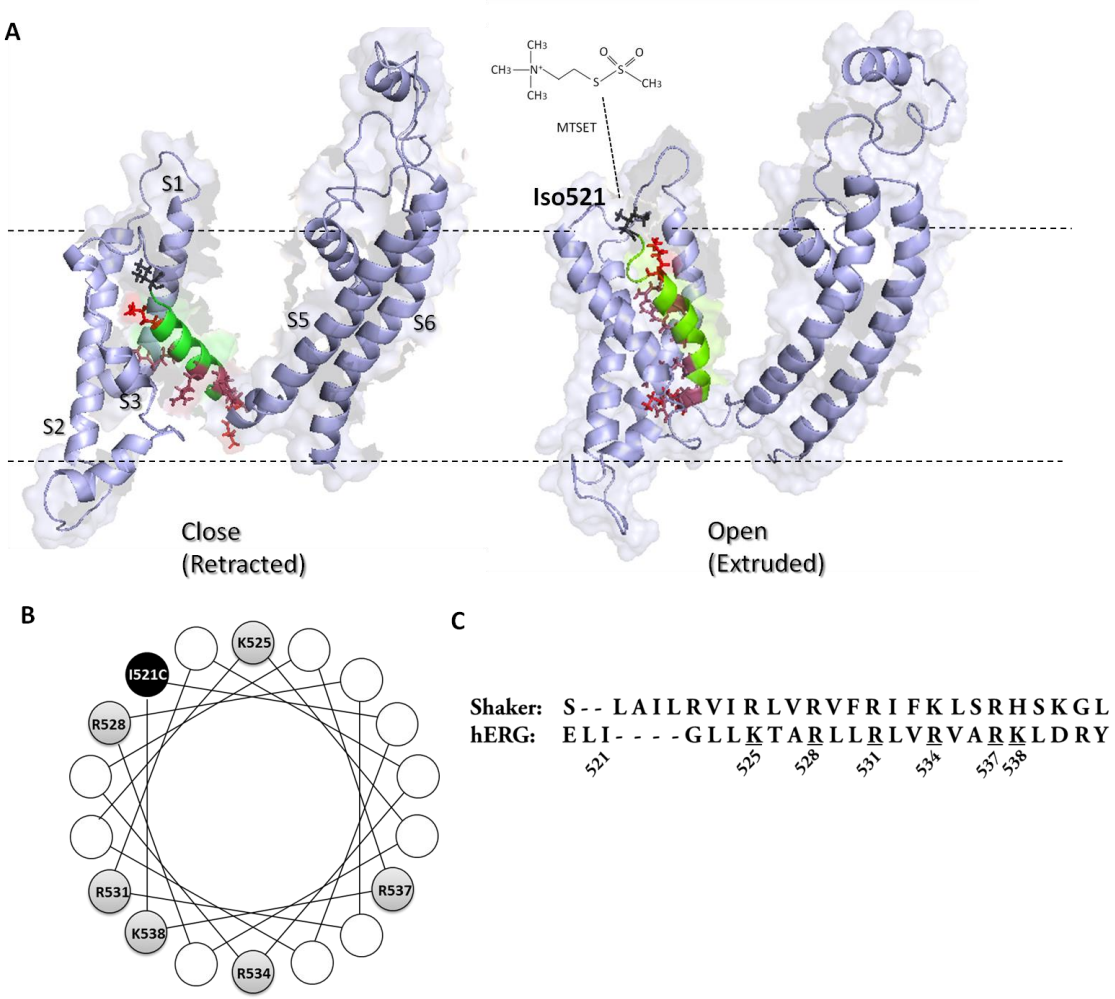

Figure 3.1 A model for the topology of a hERG single subunit.

The transmembrane segments (S1-S6) and the approximate location of positively charged residues in S4 are indicated. (A) Based on a homology model of hERG generated with Pymol (the model originally suggested by Durdagi et al. 2012), the cysteine engineered I521 (black symbol) becomes completely buried in the membrane in the closed state while S4 segments with I521C are exposed to outer MTSET in the open state (Dou et al. 2013). Positively charged residues, lysines and arginines are highlighted by red and pink symbols, respectively. (B) α-Helical diagram summarizing each residue in hERG. Cysteine-introduced at I521 on the outer side of S4 and charged residues are depicted in black and gray, respectively. Note that there is one face with the cluster of charged residues excluding R537. (C) Alignment of amino acid sequences of the S4 region for *Shaker* and hERG channels. The basic residues (K525, R528, R531, R534, R537, K538) that were mutated to uncharged residues, glutamine (Q) (Lee et al., 2009) are underlined.

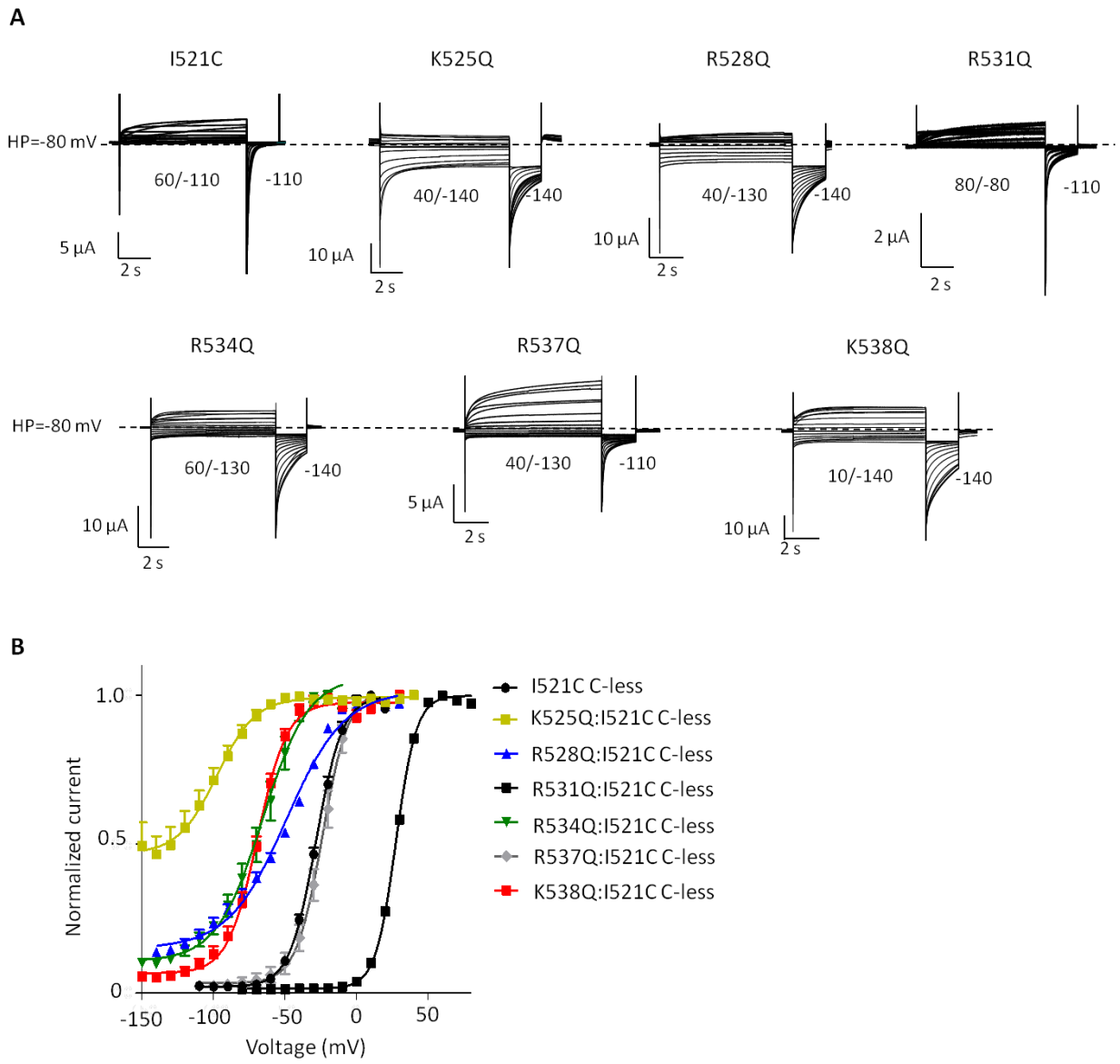

Figure 3.2 Effects of charge mutations on the voltage dependence of activation of the hERG channels.

(A) Representative currents were elicited by 8 s depolarizing steps from a holding potential of -80 mV in 10-mV increments, followed by a 2 s hyperpolarizing step to the indicated potential. (B) Normalized conductance-voltage (G-V) relationships were obtained by plotting the normalized peak tail currents for each mutant versus the preceding depolarization.

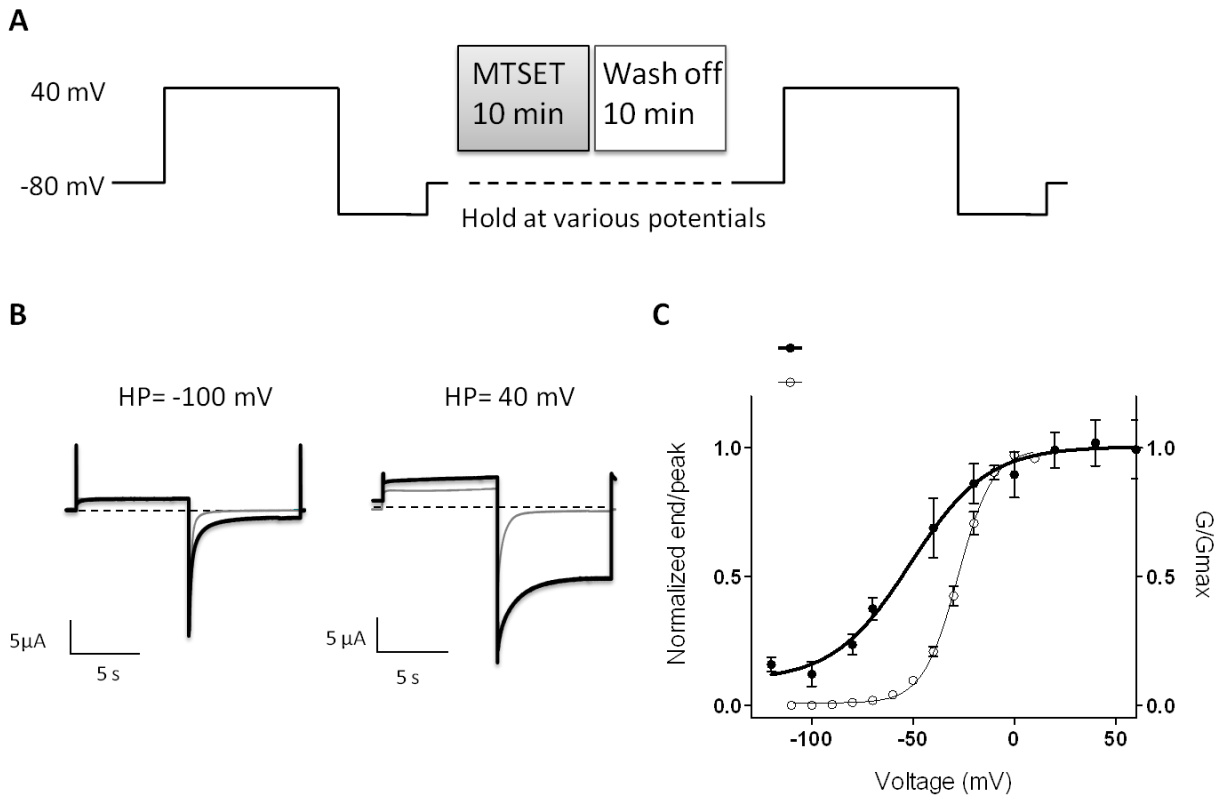

Figure 3.3 MTSET effects on I521C hERG channels.

(A) The voltage pulse protocol used to study the state-dependent modification by external application of MTSET. Currents were recorded by stepping from a holding potential of -80 mV for 8 to a test voltage of +40 mV for 8 s, followed by holding at the different voltages and then applying MTSET for 10 min. After washing residual MTSET from the chamber, we used the same protocol to measure current changes. (B) Current records are shown before MTSET application (gray) and after washout of MTSET (black) when the membrane was held at the either hyperpolarized (-100 mV) or depolarized potential (40 mV). (C) Comparison between the steady-state G-V curve and after MTSET modification. The MTSET modification curve was measured from the tail currents, calculated current amplitude at peak (filled arrow) and end (open arrow) as in B. The ratio of the end to the peak were normalized to a maximum value, and fitted with a Boltzmann function.

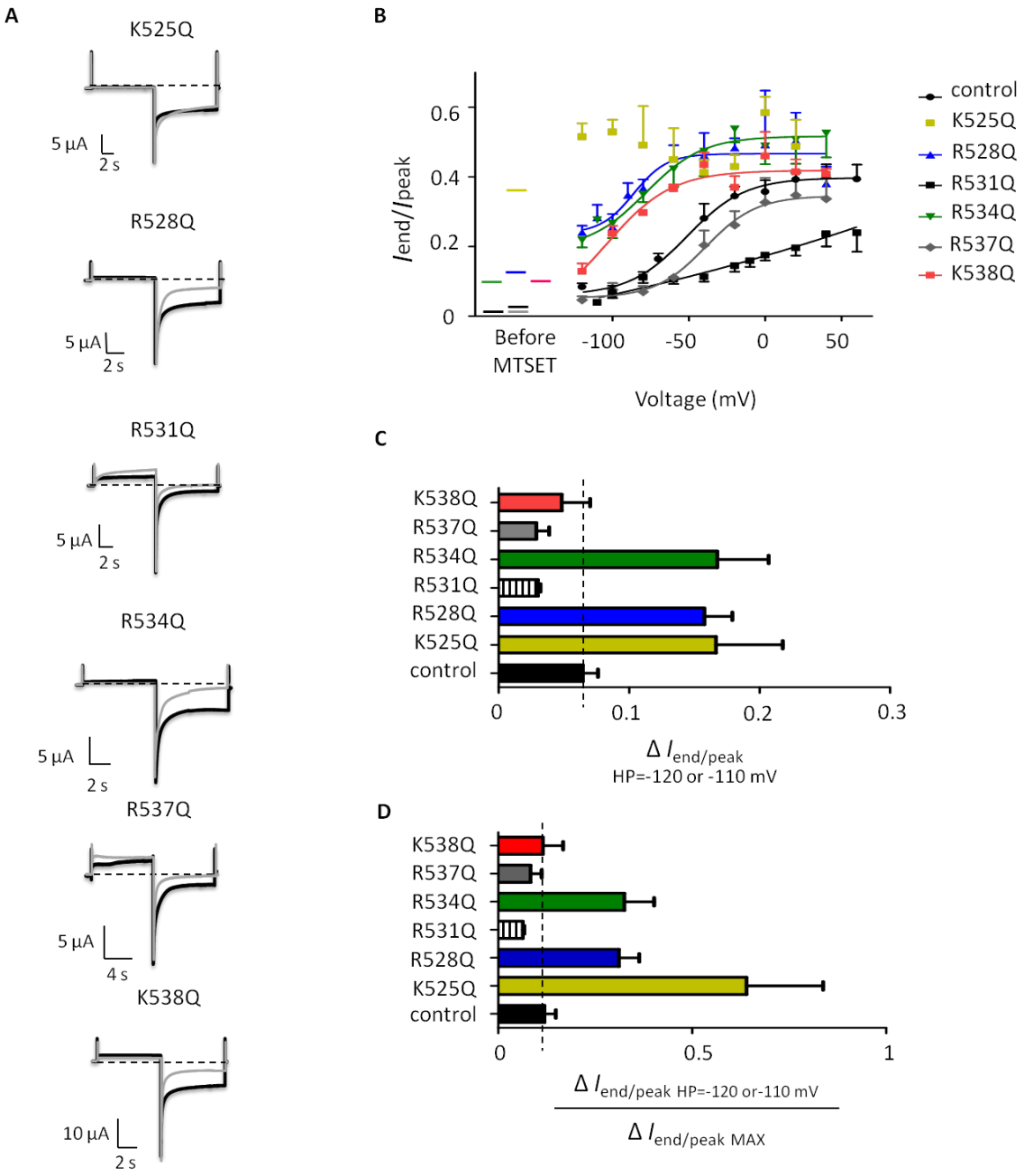

Figure 3.4 Effects of MTSET on charge mutations.

(A) The typical examples of each mutant at 100 mV before (gray) and after (black) MTSET perfusion. (B) MTSET modification-voltage relationship was measured by the magnitude of the end/peak of tail currents against holding voltages. Colored bars represent the ratio of end/peak of tail currents before MTSET. (C) Average changes in the value of Δend/peak of tail currents when the membrane potential was held at -120 mV (-110 mV for R531Q). (D) Comparison of the ratio between Δend/peak at -120 mV and the maximum Δend/peak obtained from each mutant.

Table 3.1 Steady-state activation and the voltage-dependence of S4 movement.

	Activation			S4 movement	
construct	$V_{1/2}$ (mV)	*k*	*n*	$V_{1/2}$ (mV)	*k*
I521C (control)	-28.2±1.2	9.3±0.6	4	-51.4	19.0
K525Q/I521C	-100.0±2.3	14.9±0.6	7	N/A	N/A
R528Q/I521C	-48.9±0.9	20.5±1.2	6	-83.2	11.3
R531Q/I521C	28.0±0.3	7.5±0.14	8	-19.3	25.0
R534Q/I521C	-65.7±4.5	15.0±0.6	8	-76.6	17.7
R537Q/I521C	-23.9±2.3	9.0±0.7	6	-35.5	15.4
K538Q/I521C	-58.6±1.8	11.1±0.6	7	-97.0	18.17

The data were shown as means ± SEM. N/A, not applicable.

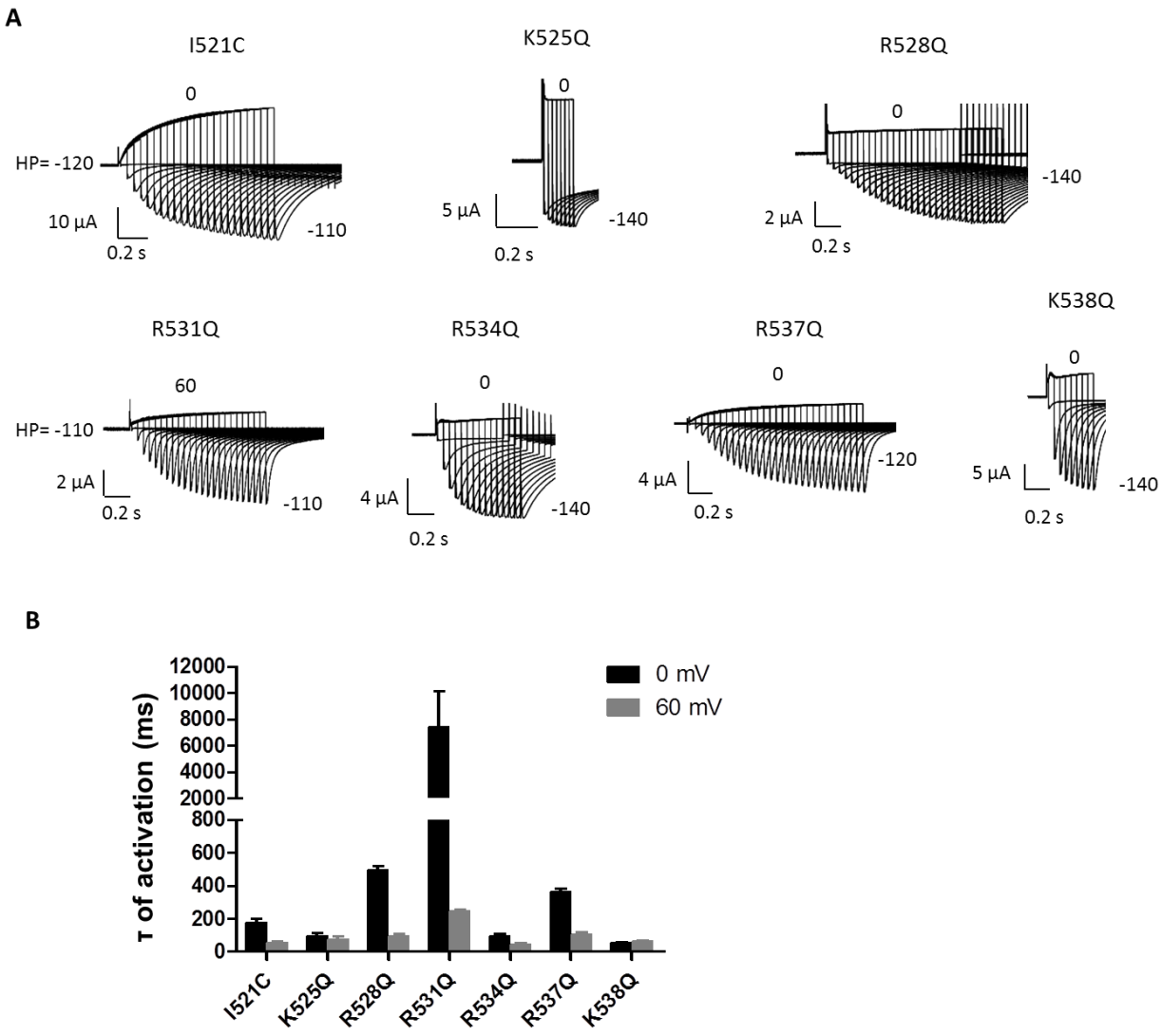

Figure 3.5 The rate of activation at 0 and 60 mV for different S4 charge mutations.

(A) Typical examples of the time constant of activation (τ) from mutations, measured by the envelope-of-tail protocol. The membrane was held at -120 mV (-110 mV, R531Q) and pulsed to 0 mV or 60 mV with 15 ms pulse, followed by increases of each sweep with 15 ms or 45 ms interval. This growth of peak tail current was fitted with a single exponential function. (B) Summary of the time constant of activation for all mutants at 0 and 60 mV (mean ± SEM, $P \leq 0.05$, ANOVA with Dunnett's method).

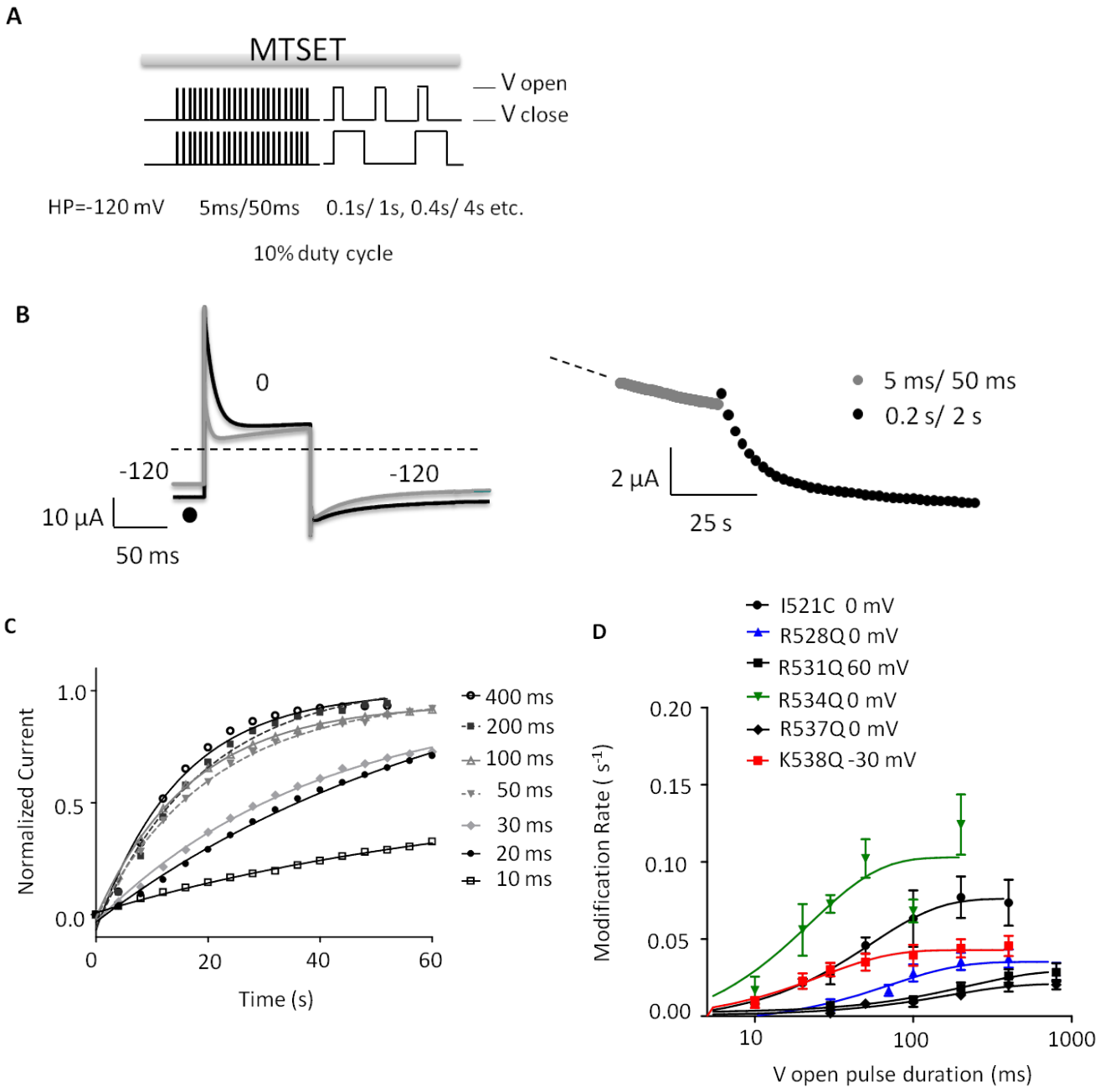

Figure 3.6 The time course of S4 movement for each of the charge mutations.

(A) The voltage pulse protocol used for measuring the time-dependent S4 movement. During the application of 1 mM MTSET, a holding potential of -120 mV (-110 mV for R531Q) was routinely used, at which most channels were completely closed. The repeated short pulses (5 ms depolarized pulse every 50 ms) were used to isolate a non-specific effect of MTSET and then oocytes were depolarized to the same voltage for 10% of the successive cycle duration (see Fig

3.6 A left : 0.1s/ 1s, 0,4s/ 4s etc.) to extract modification rates (referred to as a 10% duty cycle). Note that the depolarized and hyperpolarized membrane potentials are indicated as V open and V close, respectively. (B) A typical example recorded from I521C is shown. The magnitude of the time-dependence current was measured prior to each pulse (-120 or -110 mV) (●) where oocytes were depolarized to 0 mV for 0.2 s/2s from the beginning (gray) to end (black) of the MTSET exposure in the left panel. Representative current traces of I521C from the first set of pulses (5 ms / 50 ms, gray) to the successive set of pulses (0.2 s/ 2 s, black) are indicated in the right panel. Representative currents recorded from I521C at the beginning (gray) and the end (black) of the pulse protocol where oocytes were depolarized to 0 mV for 0.2 s/2 s are shown on the left lower panel. (C) The time course of S4 movement from the MTSET-induced increase of inward current at I521C (e.g., 1 ms per 10 ms, 2 ms per 20 ms, etc., up to 400 ms every 4 s). Averaged fits from 3-4 cells are shown overlain on the mean current data for different pulse duration protocols, which have been normalized to the maximum change predicted from the fitting, and plotted against time of total exposure to MTSET. For clarity, only selected points are plotted (Z. Wang et al. 2013). (D) The modification rate constants from each mutant for individual various pulse experiments are plotted on a logarithmic scale against the depolarizing pulse duration and were fit to the single exponential function.

Table 3.2 Effects of charge mutations on the time constants of activation and S4 movement.

construct	HP (mV)	DP (mV)	τ of activation (ms)	*n*	*τ* of S4 (ms)	Ratio: *τ* of S4 / activation
I521C (control)	-120	0	176 ± 26	4	57.0 ± 13.7	0.32
I521C (control)	-120	60	52 ± 12	4	8.5 ± 1.1	0.16
K525Q/I521C	-120	0	93 ± 21	4	N/A	N/A
R528Q/I521C	-120	0	494 ± 25	4	100.0 ± 20.1	0.20
R531Q/I521C	-110	60	247 ± 9	5	227.8 ± 87.1	0.92
R534Q/I521C	-120	0	95 ± 12	7	22.7 ± 8.5	0.24
R537Q/I521C	-120	0	364 ± 17	4	214.2 ± 80.5	0.58
K538Q/I521C	-120	0	53 ± 7	4	16.2 ± 9.2	0.31
K538Q/I521C	-120	-30	195 ± 26	4	26.5 ±9.7	0.14

The tau values of S4 movement shown in the sixth column were obtained from the holding potential (HP) and the depolarizing potential (DP) indicated in column two and three, respectively. N/A, not applicable.

Chapter 4: Residues at the inner part of the VSD that constrain S4 movement

4.1 Introduction

Upon depolarization, the VSDs undergo a conformational change to open or the close the ion permeation pathway (Bezanilla 2000). Early studies from *Shaker* channels suggested the first four S4 basic amino acids are primarily responsible for the gating charge regulating channel activation (Aggarwal and MacKinnon 1996; Fedida and Hesketh 2001; Seoh et al. 1996). These basic residues are proposed to create ion pairs with acidic residues in the neighboring S1, S2 and S3 segments and S4 outward movement are thought to be catalyzed by sequential exchange of ion pair partners (Papazian et al. 1995; Tiwari-woodruff et al. 2000).

To date, there are a few studies looking at the potential charge pairings between S4 and S1-S3 in hERG channels (Cheng et al. 2013; Piper et al. 2008; M Zhang et al. 2005). hERG's voltage-sensor, S4, has five positive charges and an extra lysine adjacent to the bottom of S4 (K538), and hERG contains six (as opposed to three in the *Shaker* channel) negative charges in the other transmembrane segments (S1-S3) of the VSD. Generally, three residues (D456 and D466 in S2, D501 in S3) are highly conserved among the members of voltage-gated potassium superfamily, whereas three others (D411 in S1, D460 in S2 and D509 in S3) are only conserved among members of the eag subfamily of Kv channels (Fig. 4.1). These additional acidic residues slow gating of the hERG channel. Using a double-mutant cycle analysis, we assessed the potential interactions between D411 and K538 at the innermost edges of S1 and S4, respectively (M Zhang et al. 2005). A previous study showed that D411 may also interact with R531 in the middle of the S4 segment (Piper et al. 2008). Both D411 and K538 residues are proposed to play a fundamental role in stabilizing the channel in the closed state and contributing to the slow rate of hERG channel activation (J. Liu et al. 2003; Piper et al. 2005; Mei Zhang, Liu, and Tseng

2004). Charge-reversal mutations on two lysines (K525D and K538D) at the top and base of S4 accelerate channel activation, but other mutations do not (M Zhang et al. 2005), emphasizing the importance of these two charged lysines in S4. To quantify the influence of the total perturbation from K538 mutations, several studies have calculated the $\Delta\Delta G$ value (K538R, K538Q, K538A and K538C), all of which showed negative $\Delta\Delta G$ perturbation indicating destabilization of the closed state relative to the open state (Cheng et al. 2013; Piper et al. 2005; Mei Zhang, Liu, and Tseng 2004). On the other hand, gating currents from K538A did not change the estimated perturbation ($\Delta\Delta G_{\text{gating}}$) for total charge movement, suggesting that K538 might be involved in channel opening rather than S4 movement itself (Piper et al. 2005). For D411, one MTSET accessibility study found that the extracellular accessibility of D411C is voltage-dependent, implying that S1 segments experience a conformational change (J. Liu et al. 2003). Although the S1-S3 segments are considered to interact intrinsically and modulate the S4 segments, few studies have focused on the role of atypical amino acids on S1. Therefore, this study will mainly investigate the contribution of the extra acidic residue, D411, and the basic K538 residue to hERG channel gating.

Changes in membrane potential drive the S4 helix motion across the membrane with the charged residues, which produce the gating current via a displacement of charged residues through the electric field (Bezanilla et al. 1991; Piper et al. 2003). It has been known that gating currents can provide better information on voltage-dependence of the transitions between closed states than ionic currents, which primarily offer information on transitions near the open state (Bezanilla et al. 1991; Santacruz-toloza, Bezanilla, and Papazian 1994). In 1997, Wang and colleagues reported a simple linear scheme of the hERG activation pathway, which included both voltage-sensitive (C_1-C_2) and –insensitive (C_2-C_3) steps preceding the open state (C_3-O) (S.

Wang et al. 1997). Upon membrane depolarization, an intramembrane charge displacement is measured by integration of either the hERG ON (Ig_{ON}) or OFF (Ig_{OFF}) gating currents elicited by depolarization or repolarization, respectively (Goodchild and Fedida 2013; Piper et al. 2003). Unique gating properties of hERG channels have two distinct components (fast and slow) which differ almost 100-fold in their kinetics (Piper et al. 2003). It is thought that slow Ig_{ON} and Ig_{OFF} result in a slow rate of activation and deactivation of the hERG ionic currents, respectively (Piper et al. 2003).

The purpose of this study is to define the influence of charge neutralizations on S1 and S4 related to hERG channel charge movement. To accomplish this goal, we measured gating and ionic currents by using cut-open vaseline gap (COVG) and two-electrode voltage clamp (TEVC) techniques, respectively. Our studies find that both K538 and D411 not only play a vital role in stabilizing the channel in the resting state, but also contribute to slowing the S4 movement through the whole activation process. Also, the comparison of the regulation of S4 movement and pore-coupling may offer insights into the interaction between K538 and D411. Our results show that the Q-V relationship of D411N does shift considerably leftward but there is a minor change in the *G-V* relationship.

4.2 Effect of neutralization on activation parameters

To test the hypothesis that neutralized K538 and D411 disrupt an essential constraint, which affects the channel stabilization in the closed state, we replaced K538 and D411 with a neutral amino acid, glutamine (Q) and asparagine (N) within the I521C background, respectively. For simplicity, the indication of I521C: C-less background is omitted in this chapter. Typical data from each mutant, double mutants, and control (I521C) are depicted in Fig 4.2 A. To estimate the

half-maximum activation voltage ($V_{1/2}$) and the slope factor (k), the voltage dependence of activation curves are characterized by plotting the peak tail currents against the preceding voltages and fitting data to a Boltzmann function (Fig 4.2 B). First, K538Q shifts the activation curve by about -30 mV. On the other hand the position of the *G-V* for D411N was almost unchanged, although both K538Q and D411N slightly changed the slope of the G-V curve compared with control (Table 3). Changing the charge on the voltage sensor might be expected to alter the slope factor of K538Q and D411N. In Chapter 3, we measured the voltage dependence of channel activation for R537Q (one residue above K538), and found little change in its properties ($V_{1/2}$ = -23.9 ± 2.3, k = 9.0 ± 0.7) compared with control ($V_{1/2}$ = -28.2 ± 1.2, k = 9.3 ± 0.6). This suggests that K538 has a superior contribution to the stabilization of the closed states than R537 on the intracellular side of S4 charged residues.

We also made a double mutant to confirm the ion pairing between D411N and K538Q. The original current traces and data are summarized in Fig 4.2 and Table 3. As with charge-reversal mutations of these residues (M Zhang et al. 2005), the D411N/K538Q activation curve almost superimposes on the activation curve for K538Q alone. One reasonable approach to quantifying the coupling of mutations during channel activation, is double-mutant cycle analysis (Li-smerin, Hackos, and Swartz 2000; Yifrach and Mackinnon 2002; M Zhang et al. 2005). We calculate the absolute value of nonadditivity ($\Delta\Delta G_{\text{coupling}}$) using ΔG_0 value from single and double mutants as illustrated by the thermodynamic box in Fig 4.2 C. The effects of mutation 1 and mutation 2 are not additive if two residues are energetically coupled, then the degree of nonadditivity will exceed ~ 4.2 kJmol^{-1} (Yifrach and Mackinnon 2002; M Zhang et al. 2005). For our D411N/K538Q pair, the nonadditivity value is 7.5 ± 0.5 kJmol^{-1} (Table 3). This result confirms

that the effects of mutations at position D411 and K538 are functionally coupled, which is consistent with the study of charge reversal mutations (D411K/K538D) (M Zhang et al. 2005).

4.3 Gating currents measurement

Using the COVG technique, we recorded hERG gating current for D411N, K538Q and control (I521C), and their representative currents are shown in Fig 4.3 A. For I521C (control) the OFF gating currents (Ig_{OFF}) are elicited by repolarization to -110 mV for 100 or 300 ms after multiple depolarizing pulses for 100 or 300 ms in 10 mV increments. Due to the fast kinetics of activation, normally a 24 or 100 ms protocol is used for K538Q and D411N mutations. The integral of Ig_{OFF} referring to the charge (Q) plotted against voltage is defined as the Q_{OFF}-V relationship, fitted with the Boltzmann function (Fig 4.3 B). In all constructs, the Q-V (gating charge movement) curves are placed at more hyperpolarized potentials than the G-V (ionic conductance) curves, implying that the charge movement during voltage-dependent transitions occurs between closed states in the activation pathway before channel opening (Bezanilla et al. 1991; Santacruz-toloza, Bezanilla, and Papazian 1994).

The gating currents of mutations D411N and K538Q demonstrate differences from those of control. The Ig_{ON} of the control has a fast component followed by a slow component consistent with WT hERG gating currents where two elements are clearly distinguished (Goodchild and Fedida 2013; Piper et al. 2003). However, the existence of two components of gating charge movement is eliminated by either the D411N or K538Q mutations (Fig. 4.3 C). Compared with the Q_{OFF}-V relationships of control ($V_{1/2}$ = -25.9 ± 1.8, n = 4), both D411N ($V_{1/2}$ = -37,8 ± 0.9, n= 3) and K538Q ($V_{1/2}$ = -35.6 ± 1.8, n = 4) show a negative shift of the midpoint of Q_{OFF}-V curves, suggesting that their S4 domains required less energy to traverse the membrane.

4.4 Effects of mutations on the kinetics of hERG ionic activation and charge movement

We used an envelope of tails current protocol to define the impact of mutations on the kinetics of hERG channel activation and charge movement with TEVC and COVG techniques, respectively. Like *Shaker* channels, hERG channels experience several closed states in the activation pathway, and an envelope of tails current protocol was used to measure the rate of channel activation; the envelope-of-tails analysis avoids complications that arise when the rapid inactivation process overlaps the activation process (Fig. 2.1 B) (S. Wang et al. 1997). Representative original traces for ionic activation and gating charge movement are shown in Fig 4.4 A, B.

For time constants of channel activation, both D411N and K538Q show a faster rate of activation at 0 mV than control, which is consistent with neutralization studies of these mutations (D411C, K538Q) (Cheng et al. 2013; J. Liu et al. 2003). To clarify the effect of D411N and K538Q on the S4 movement, we first characterize the time constant of charge movement on these mutations. The integrals of Ig_{OFF} plotted against increasing time are well-fitted with a single exponential curve (Fig 4.4 C). It is evident that these mutations speed up channel opening. Additionally, the gating current measurements indicate that both charge-neutralizing mutations in the innermost of S4 cause a faster rate of charge movement than control (control τ = 46 ms). Even D411N (τ = 17 ms) mutations cause a greater effect on S4 movement than K538Q (τ = 23 ms). This result suggests that both neutralizing mutations potentially cause the acceleration of total charge movement.

Next, we summarize the values of time constants from each construct to determine the kinetic relationship between channel opening (ionic) and charge movement (gating) (Fig 4.5). Early studies revealed that hERG channels experience a voltage-independent step at very positive

potentials preceding the concerted opening step (Subbiah et al. 2004; S. Wang et al. 1997). Consistent with hERG WT gating kinetics (Goodchild and Fedida 2013), we observe a voltage-independent step at positive potentials on both the time-constants of channel activation and time-constants of charge movement, both of which saturate at the same positive potentials greater than +40 mV (Fig 4.5 A). On the other hand, time constants for charge movement of D411N and K538Q continue to increase at more depolarized potentials, which does not parallel with the rate of channel opening (Fig 4.5 B, C), implying that effects of both mutations on S4 movement is separate from their effects on the voltage independent step.

4.5 Discussion

Based on the alignment with the archetypical *Shaker* K^+ channel (Lee er al. 2009), hERG shares the highly conserved negative charges in S1 – S3 and has three additional acidic amino acids in S1 – S3 (D411, D460, and D509). Besides, hERG has two lysines in the outer and innermost regions of the S4 domain (K525 and K538), which contribute to the stabilization of the channel in the closed state relative to open state as described in Chapter 3 (Cheng et al. 2013; Subbiah et al. 2004). Using tryptophan-scanning mutagenesis, some authors have proposed that K525, R528, and K538 are the main molecular determinants of the movement of the hERG S4 helix (Subbiah et al. 2005). One charge-interaction study proposed the potential for salt bridge formation between D411 and K538, which may regulate the downstream channel activation process (M Zhang et al. 2005). However, the question of why the kinetics of the hERG channel are so different from other Kv channels is not entirely answered. Consequently, the primary goal of this study was to address the role of two charged residues in the innermost of the channel--D411 and K538 - on the regulation of S4 movement.

The principal findings of this study can be summarized as follows. First, the neutralizing mutation on the D411, which is an additional acidic residue unique to hERG channels, shows unusual gating properties. D411N mutations have a significant left-shifted *Q-V* curve although its *G-V* curve is a little shifted compared to the control. To test the influence of the I521C background, we examined gating currents of D411N mutations without I521C, which resemble those of D411N with I521C background. This suggests that the I521C background has little influence on the effects of D411N gating current data (see Appendix, Fig A.3). Plus, removing the charge at position 411 drastically accelerates the rate of S4 movement and channel opening. As opposed to other extra acidic residues (D460 and D509), only D411 mutations expedite the rate of channel activation among three non-conserved negative residues (J. Liu et al. 2003), highlighting the significant contribution of D411in the stabilization of the channel in the resting state. Second, K538Q mutations not only shift the G-V relation far to the left, but also they alter the Q-V curve to the left, causing the rapid kinetics of S4 movement and channel activation. Collectively, two charged residues in the intracellular region contribute to the stability of the channel and S4 in favor of the resting state, but different properties between the two residues on S4 movement and pore-coupling are observed.

In this study, a simplified 2-state gating model was used to calculate the absolute changes in the energetics of channel gating by mutations (data summarized in Table 3 and 4). This is, of course, limited in its relevance to physical reality due to the presence of multiple transitions in the activation pathway (Subbiah et al. 2004; S. Wang et al. 1997). Nevertheless, it can be an effective way to illustrate potential parameters affected by mutations, and how channels are easy or difficult to open or close related to membrane depolarization or repolarization, respectively (Cheng et al. 2013; Li-smerin, Hackos, and Swartz 2000; Piper et al. 2008; M Zhang et al. 2005).

To visualize the effect of D411N and K538Q mutations through the whole activation process, a linear gating scheme for hERG was utilized without an inactivation process for simplicity, and is depicted in Fig 4.6 (S. Wang et al. 1997). This diagram is based on the idea that the channel traverses several closed states (C_1-C_2-C_3) measured as gating currents before channel opening (O), which is reflected by ionic current measurement (Bezanilla et al. 1991; Santacruz-toloza, Bezanilla, and Papazian 1994). For the time constant of charge movement and ionic conductivity, the transitional kinetics linking individual states are depicted as the height of energy barriers. For instance, an increase in the rate can be described as the reduction of the energy barrier and vice versa. At the C_1 state, the leftward shift of the *Q-V* curve implies the destabilization of the resting state depicted as red and blue lines for D411N and K538Q, respectively. The faster kinetics of S4 movement of both mutations rather than control (black line) is reflected in decreasing the energy barrier for $C_1 \rightarrow C_2 \rightarrow C_3$ transitions. Interestingly, although D411N mutations greatly accelerate the rate of channel activation (C_3-O), they do not alter its *G-V* curve. It may due to the faster rate of deactivation of D411N mutations. On the other hand, the left shift of the *G-V* curve and the faster τ for K538Q compared with the control is consistent with other studies (Cheng et al. 2013; Mei Zhang, Liu, and Tseng 2004). This phenomenon may be described as no change in the C_3 state for D411N and the destabilization of the C_3 state for K538Q. The faster kinetics with K538Q may be achieved by decreasing the depth of the energy well in individual transitions.

It has been suggested that hERG channels have a voltage-independent step (C_2-C_3) right before reaching the opening state (Subbiah et al. 2004; S. Wang et al. 1997). During this rate-limiting step the kinetics of hERG S4 movement become consistent with the rate of channel opening at positive potentials, and fail to increase with further depolarization. This implies that

the step reflects intrinsic S4 limits rather than the opening transitions downstream (Goodchild and Fedida 2013; S. Wang et al. 1997). However, in Fig. 4.5 we summarize the kinetic relationship between ionic and gating current in D411N and K538Q and show that these mutations removed the limitations on S4 charge movement at positive potentials, but did not affect the overall voltage independent step of channel opening. The regulation of S4 movement by D411N and K538Q is dissociated from pore-opening at very positive voltages. This also suggests that constraints imposed by D411 and K538 normally play a pivotal role in controlling the kinetics of total charge movement in hERG channels.

In summary, we first demonstrate an important contribution of acidic charge D411 to the kinetics of charge movement and channel activation. Although there is no direct evidence to show a direct molecular interaction between K538 and D411, neutralizing D411 caused S4 gating charge movement to become significantly faster. Therefore, it seems likely that D411 interactions with K538 are more prominent in the closed conformation and contribute to slow overall S4 movement.

4.6 Figures and Tables

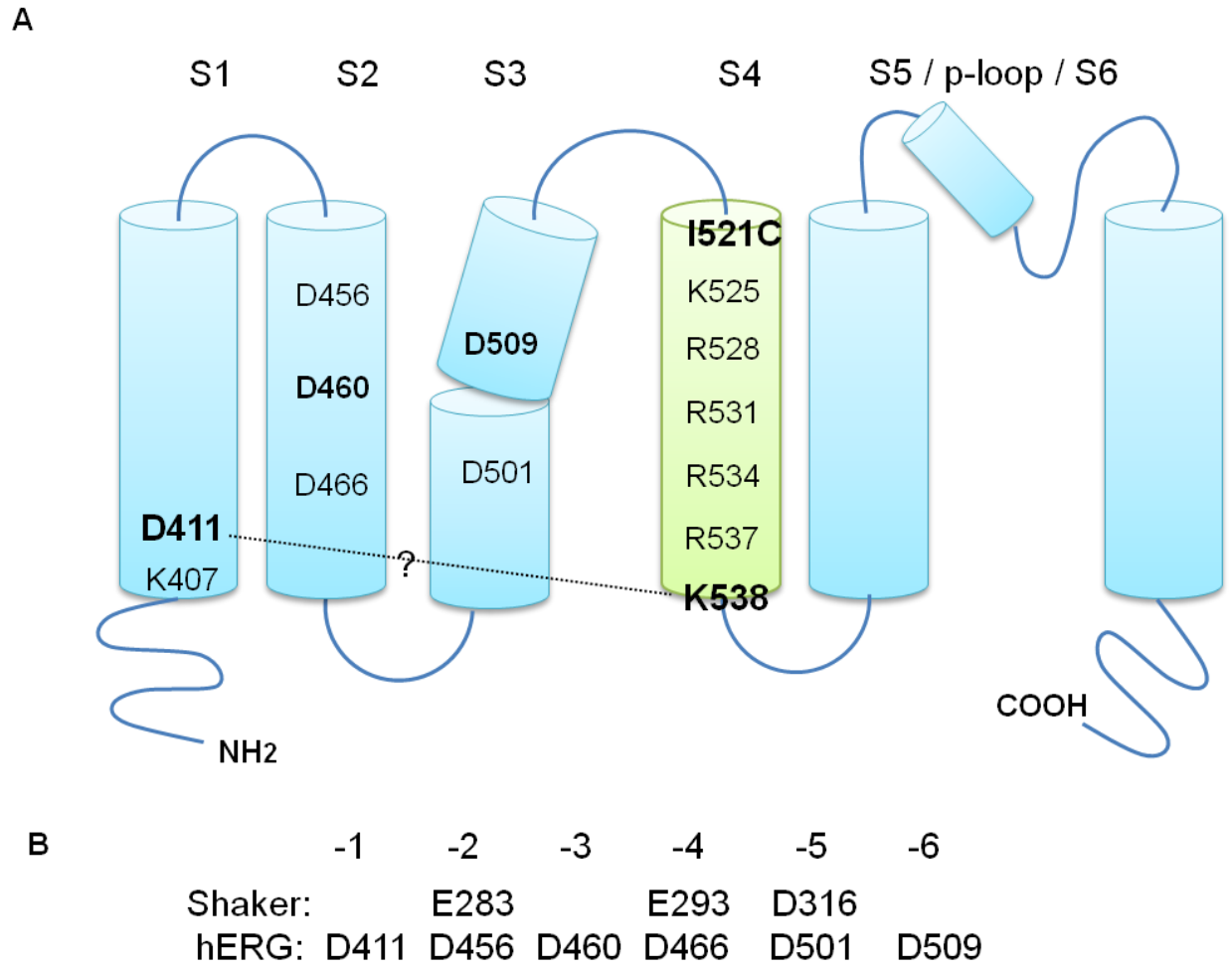

Figure 4.1 Topology of potential interaction between D411 and K538.

(A) Residues and position numbers for the acidic (S1-S3) and basic residues (S4) in the VSD. Aspartate residues were indicated in S1-S3, where non-conserved aspartate residues in hERG channels are highlighted in bold. A potential interaction between D411 and K538 was suggested in the previous study (M Zhang et al. 2005). (B) Comparison of residues and positions of negatively charged residues between *Shaker* and hERG channels: E283, E293, and D316 in the S2-S3 domain of *Shaker*. There is only one acidic residue in S1 of hERG (D411). Alignment of negatively charged (acidic) residues for hERG and *Shaker* based on the alignment software (Liu et al. 2003).

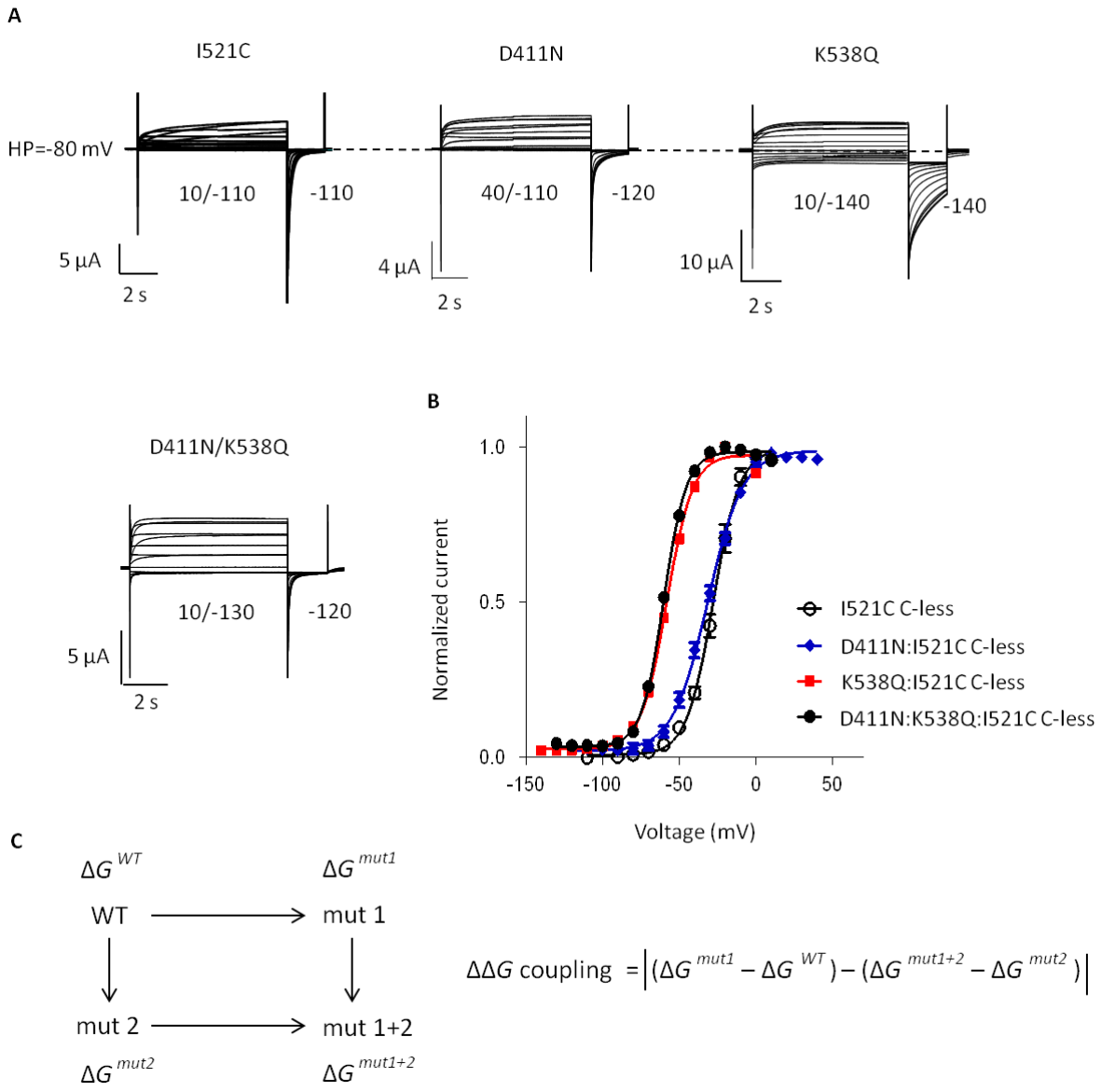

Figure 4.2 Effects of single and double charge neutralizing mutations of D411 and K538 on the voltage-dependence of hERG activation.

(A) Currents elicited by the indicated voltage pulse protocol used to determine activation parameters. (B) Normalized current-voltage relationships for single and double mutant hERG channels elicited by Boltzmann function. (C) Left panel: The free energy of channel activation at 0 mV (ΔG) of WT, single mutant (mut1 or mut2), and double-mutant (mut 1 + mut 2) channels are depicted as a diagram. Right panel: The value of nonadditivity ($\Delta\Delta G$ coupling) is calculated as the absolute value of the difference between the effect of mut1 in the I521C background versus that effect measured with the mut2 in the I521C background (Li-smerin, Hackos, and Swartz 2000; M Zhang et al. 2005).

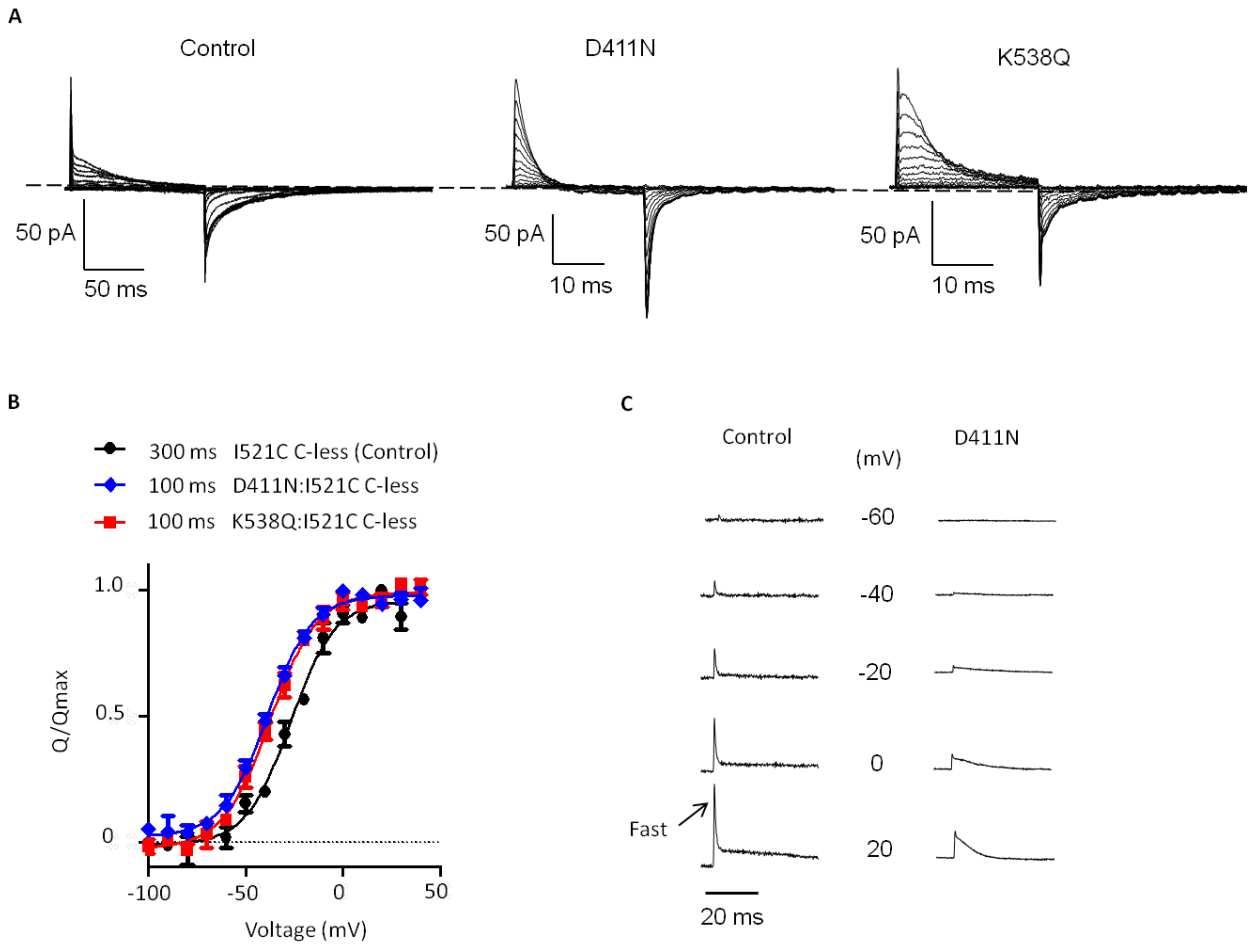

Figure 4.3 Effect of charge mutations on the voltage dependence of gating charge movement.

(A) The typical examples of gating currents elicited from Control (I521C), D411N, and K538Q mutant hERG channels. The membrane potential was applied from a holding potential at -110 mV to a range of test potentials for 100 ms for control and 24 ms for D411N and K538Q, respectively. Off-gating currents were integrated over a 300 ms interval for control traces and 100 ms for D411N and K538Q. (B) Normalized Q_{OFF}-V relationship of control and each mutant. The integrals of Ig_{OFF} currents against test voltage were fit with a Boltzmann function. (C) Representative traces at the indicated potentials from control and D411N. Fast and slow components of gating charge movement overlap in D411N, but are separated in the hERG channel (Goodchild and Fedida 2013; Piper et al. 2003).

Table 4.1 Double mutant cycle analysis on activation gating of the hERG channel.

Construct	$V_{1/2}$ (mV)	k (mV)	ΔG (kJmol^{-1})	$\Delta\Delta G_{coupling}$ (kJmol^{-1})	n
Control	-28.2 ± 1.2	9.3 ± 0.6	-7.5 ± 0.6	N/A	4
D411N	-31.0 ± 1.0	11.7 ± 0.5	-6.5 ± 0.2	N/A	3
K538Q	-58.6 ± 1.8	11.1 ± 0.6	-13.1 ± 0.7	N/A	7
D411N/K538Q	-59.9 ± 1.0	7.5 ± 0.2	-19.9 ± 0.4	7.8 ± 1.1	3

$V_{1/2,}$ the half-activation potential, and k, the slope factor, were obtained from Boltzmann fits (± SEM). The voltage-clamp protocols are described in Fig 4.2. k is equal to RT/zF, where z is the ion valency, F is Faraday's constant, R is the universal gas constant, and T is the absolute temperature. The free energy of channel activation (ΔG) = $zF \cdot V_{1/2}$ (Li-smerin, Hackos, and Swartz 2000) (± SEM). The SE value for $\Delta\Delta G_{coupling}$ was calculated as the square root of the sum of the squares of SE values for individual ΔG_0. Non-additivity was defined as a $\Delta\Delta G_{coupling}$ above 4.2 kJmol^{-1} (Cheng et al. 2013; M Zhang et al. 2005).

Table 3.2 Charge movement parameters from the normalized Q_{OFF}-V relationship.

Construct	$V_{1/2}$ (mV)	k (mV)	ΔGq (kJmol^{-1})	n
Control	-25.9 ± 1.8	10.6 ± 0.5	-6.0 ± 0.3	4
D411N	-37.8 ± 0.9	11.6 ± 0.7	-8.0 ± 0.7	3
K538Q	-35.6 ± 1.8	11.7 ± 0.7	-7.5 ± 0.5	4

Normalized Q_{OFF}-V relationship was obtained by plotting the integral of Ig_{OFF} (Q) against the test potential. The free energy of intramembrane charge movement (ΔGq) = $zF \cdot V_{1/2}$ (Li-smerin, Hackos, and Swartz 2000) (± SEM).

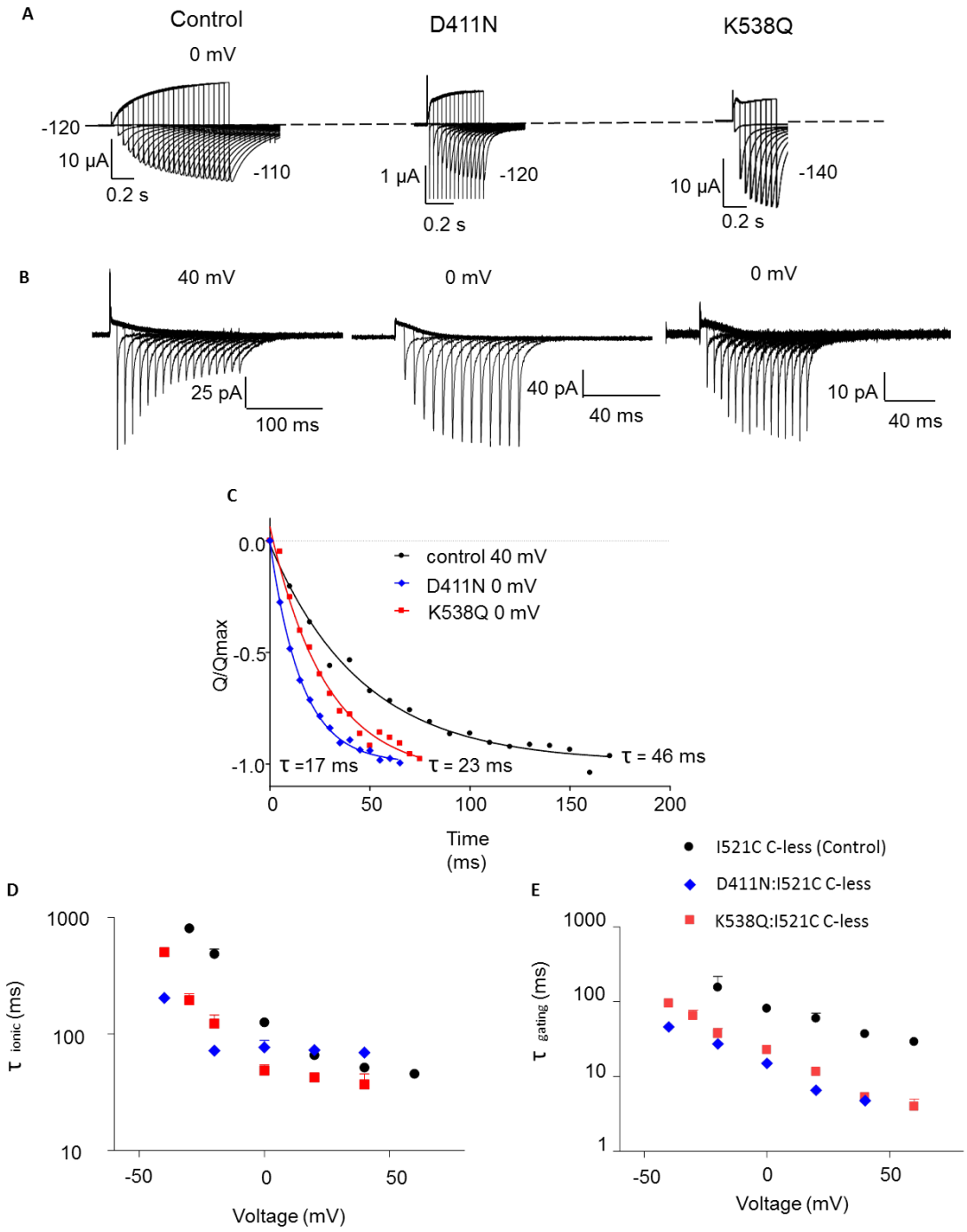

Figure 4.4 Effects of substituting neutral residues on kinetics of ionic activation and charge movement in the hERG channel.

(A) Representative current traces for each mutant and control were pulsed for a varying duration to 0 mV, followed by a repolarizing pulse at -120 mV. (B) The original traces of gating currents elicited by steps to 40 mV extending in 10 ms intervals for control and 0 mV extending in 5 ms

intervals for D411N and K538Q. (C) The integrals of Ig_{OFF} elicited by a repolarizing pulse after increasing durations of depolarizing pulses are fitted with a single exponential function. Summary of the time constants for (D) ionic current activation and (E) gating charge movement of D411N and K538Q were elicited by an envelope of tails current protocol at depolarized potentials from -40 to 60 mV.

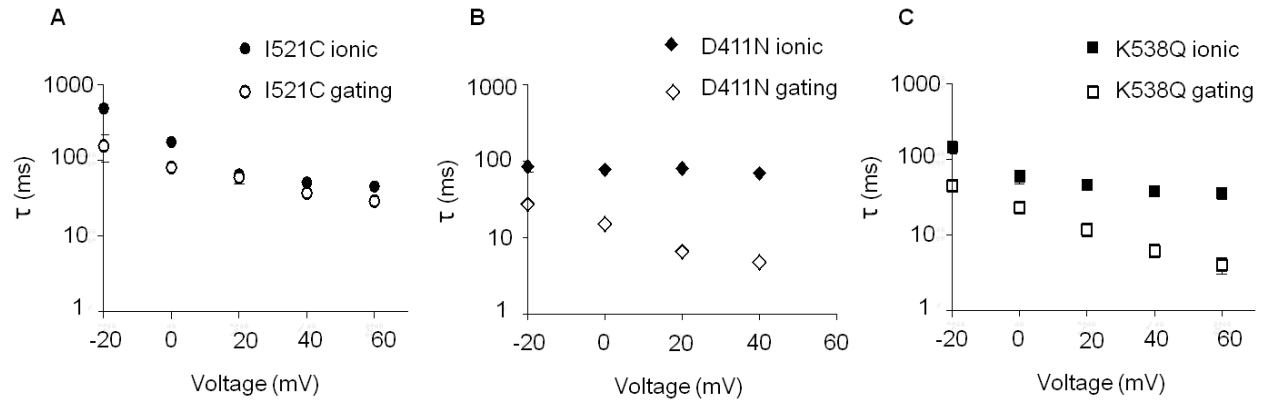

Figure 4.5 Effects of D411N and K538Q on the kinetics of channel opening and S4 movement.

(A-C) The plot of time constants of ionic and gating currents with single exponential fits from -20 to +60 mV for each mutation. The filled symbol represents the time constant of channel opening while the open symbol indicates the time constant of charge movement for each construct. The association between ionic and gating kinetics converged at more depolarized potentials for I521C while it showed the divergence for D411N and K538Q.

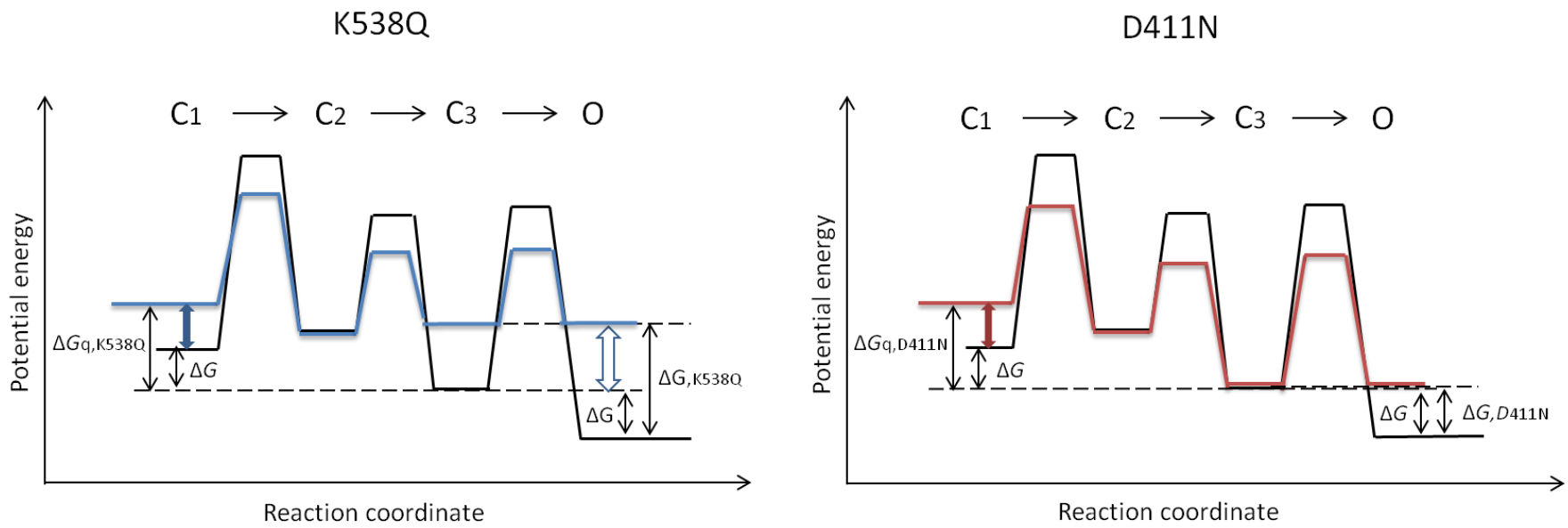

Figure 4.6 Hypothetical diagram of energy profiles for K538Q and D411N at 0 mV.

Hypothetical energy profile for K538Q (blue line) and D411N (red line) during channel activation, drawn with gating charge movement as the reaction coordinate based on the simple linear gating scheme (Cheng et al. 2013; S. Wang et al. 1997). Past studies defined that the channels have several closed states (C_1-C_2-C_3) measured as gating currents before channel opening (O), which is reflected by ionic current measurement (Bezanilla et al. 1991; Santacruz-toloza, Bezanilla, and Papazian 1994). Note that the inactivated state is excluded for simplicity. The changes between individual states are principally linked by kinetic transitions in the activation pathway (reflecting data in Fig.4.4). The fast rate of transitions is considered as a lower energy barrier between each state. The black line represents the free energy profile for control. Estimated perturbations in ΔG ($\Delta\Delta G$) were measured by the following the equation: $\Delta\Delta G = \Delta G$ mutation – ΔG control (M Zhang et al. 2005). K538Q has a greater $\Delta\Delta G$ on *G-V* (empty allow) than *Q-V* (filled arrow) relation whereas D411N has a greater $\Delta\Delta G$ change on *Q-V* (filled arrow) only.

Chapter 5: Conclusion

It is widely acknowledged that an outward displacement of the VSD (S1-S4) is coupled to opening of an activation gate (Michael C Sanguinetti and Tristani-Firouzi 2006). Among all Kv channels, positively charged residues in the fourth transmembrane segment (S4) are the principal molecular determinants of activation gating, which contains multiple regularly spaced basic residues. The hERG S4 includes one lysine and four arginines at every third position in the alpha-helix (K525, R528, R531, R534, R537) followed by one lysine adjacent to S4 (K538). Many studies have shown how individual charges affect channel activation through the approaches of mutagenesis and macroscopic ionic recordings. The first three charges (instead of the four in *Shaker*) apparently mainly contribute to gating charge (Subbiah et al. 2004; M Zhang et al. 2005), but these studies were only of ionic currents. Testing the properties of S4 motion as carried out in this thesis can allow further insights into the whole process of activation. If the channel only had two transition states (closed or open), then macroscopic ionic recording would be enough to offer information about the voltage dependence of the transition; however, the hERG channel demonstrates multiple transition states, and macroscopic current recordings are inadequate to fully understand the properties of transitions between multiple closed states.

In order to better understand the S4 movement of hERG, previous studies in our lab have developed an alternative voltage sensor assay by applying the sulfhydryl-specific chemical compound MTSET to the cysteine-introduced I521 at the top of S4 so that we are able to observe the state-dependent modification of I521C hERG channel, which directly reflects the motion of the S4 helix (Dou et al. 2013; Z. Wang et al. 2013). The studies in this thesis were designed to address the molecular basis of charge-carrying residues underlying the slow hERG gating. To accomplish this goal, we measured ionic and gating currents to determine: (i) the state-dependent

accessibility of cysteine substituted in I521 with MTSET and (ii) the gating charge movement with the COVG technique. The primary success in these studies was to elucidate the role of charged residues in S4 motion with two different approaches. Here, we first demonstrate the fundamental role of K538 in the kinetics of S4 segments with both methodologies. Especially, we first characterize the time dependence of total charge movement of acidic residues D411 on S1, which form a salt bridge with K538. Neutralization of D411 and K538 will significantly accelerate total charge movement, which suggests both residues may play an essential role in modulating the S4 movement.

The first project was designed to track S4 movement alone with the cysteine-specific binding compound, MTSET. Characterization of the properties of the control channel (I521C in this thesis) is critical to form the basis for comparison with mutant channels. Our results of the control on the time course of S4 movement with MTSET were consistent with the time dependence of total charge movement, indicating that this assay is reliable to test the movement of the S4 helix. To define the effect of S4 neutralized residues on the pattern of reactivity of I521C was one of the tasks. Our observations indicate that the glutamine mutations for K525, R528, and R534 of S4 are partly extruded, even at very negative potentials, leading to profound destabilization of S4 in its normal resting position. In light of the time course required for S4 to reach equilibrium, we observed slow S4 movement caused by neutralizing 3 residues (R528, R531 and R537), suggesting that these basic residues intrinsically favor S4 transition from the resting to active states. Among these mutations, R531Q showed the largest impact on the S4 movement. On the other hand, only K538Q accelerates S4 movement with a minor influence on the rate of pore opening, indicating an essential regulation of this residue on the S4 helix in the resting conformation.

The functional role of the charged residues in S4 in the resting position remains to be determined. In the second project, we further investigated the properties of K538 and its potential partner D411 in the S1 helix by measuring total charge movement with the COVG technique. We observed that K538Q speeds up the kinetics of total charge movement in agreement with the MTSET data. Here, we first demonstrate that D411 makes a significant contribution to the slowing of voltage sensor movement. With the two-electrode voltage clamp (TEVC) and the cut-open vaseline gap (COVG) techniques, we examined the effect of neutralizing mutations at positions D411 and K538 located in the C-terminal ends of S1 and S4, respectively, so that the results could be interpreted in light of the relationship of ionic conductance and gating charge movement. We found that both D411N and K538Q showed a left-shift of the charge-voltage relationship (*Q-V*) and exhibited faster kinetics of charge movement than the control, implying that both residues play an essential role in regulating the normal S4 movement in the hERG channels. Although a previous study (Piper et al. 2005) suggested that K538 mainly contributed to coupling voltage sensor movement to pore opening, we found that K538 also regulated S4 movement itself. Interestingly, D411N showed a hyperpolarized shift of *Q-V* with little influence on its *G-V* curve while K538Q exhibited a left-shift of both the *Q-V* and the *G-V* curve. This suggests different consequences of the two mutations during S4 movement and pore opening. The rate of charge movement in control at physiologically relevant potentials was much faster than the rate of channel opening, but S4 movement became saturated at higher depolarized potentials, indicating the presence of a voltage-insensitive step along the whole activation pathway as suggested in hERG WT channels (Goodchild and Fedida 2013). However, the kinetics of charge movement of both D411N and K538Q did not saturate even at very high potentials (Fig 4.5 B, C). It is likely that both mutations still allowed complete S4 movement at

higher depolarized potentials where the speed of channel opening becomes saturated. To depict the effects of both mutations, we applied a simple linear kinetic model through the whole activation process by using a reaction coordinate diagram (Cheng et al. 2013; Subbiah et al. 2004; S. Wang et al. 1997). The destabilization of a closed state ($\Delta\Delta G$) and the decrease of the energy barrier (faster τ) than control demonstrate how both mutations accelerate the activation process. For D411, it is possible that the high density of negative charges in hERG slows charge movement by forming more electrostatic interactions with positive charges. A change of the aspartic acid to asparagine could also cause conformational changes, making it difficult for D411N to come close to the S4 segment.

Although we demonstrated the role of D411 and K538 in the gating charge movement from the resting state, we cannot rule out the possibility that D411 might interact with other potential residues near K538, which might contribute to the downstream events. There is no direct evidence to determine the coupling between residues except the double-mutant cycle analysis we carried out, and the calculated free energy of a simplified two-state gating model. It will be interesting for future studies to understand whether electrostatic attraction between D411 and other residues in the S4-S5 regions also alters the coupling of voltage sensors to pore gates. Alternatively, the oxidation of introduced cysteine interactions or other approaches could be adopted to investigate electrostatic interactions with residue D411 (Papazian et al. 1995). Furthermore, the charge-conserving mutations, such as D411E or K538R, could provide a structural basis for modeling the movement of these residues to support our interpretations.

However, with respect to further investigations of this nature, several problems became apparent during our experiments. The measurement of the gating charge movement is challenging due to the painfully low rate of success in recording. As the gating charge movement

occurs according to voltage changes, the gating current generally has lower magnitudes than ionic current flowing via the open channel (Bezanilla et al. 1991). For success in recording the gating current, not only does a membrane need to contain a sufficient density of mutant channels but also both the ionic currents must be totally blocked and the capacitive current removed (Bezanilla 2000). The inherent difficulty of gating recording at the pinpoint of the oocyte where the membranes have enough accumulation of the mutant channels needs to be overcome. It is better to record at the black animal poles where we can identify the injection point after a few days incubation, but the high level of cRNA injection may cause severe damaging effects on oocytes depending on the construct of mutations. As chemical chaperones, small molecules (e.g., glycerol, DMSO) are thought to rescue the trafficking of mutant channels, which may provide the high expression of mutations (Gong et al. 2004; Vandenberg et al. 2012). Moreover, hERG channels blockers, such as E-4031, terfenadine, or dofetilide, could rescue trafficking defects by binding to the channel pore (S. Liu et al. 1996; Vandenberg et al. 2012). Since most drugs were tested in mammalian cells, to determine the reliable concentration of these candidates in oocytes could be one of the tasks in a future study.

In previous studies, the gating current measurement of alanine-substitution on K525 and R528 showed no functional expression (Piper et al. 2005). MTSET modification of I521C enables us detect the effects of most charged mutations on the motion of S4 helix with if they have reasonable expression. Hopefully, this advance will offer new options to understand the influence of mutations on S4 movement. Nevertheless, I521C proteins caused conformational changes if the mutations were close to its position as shown in double mutations (K525Q: I521C) for comparison with a single mutation (K525Q) (Fig A.1). As well, experiments on the time

course of S4 movement required repeated experiments on separate oocytes, so it took a long time to obtain complete current-voltage relationships.

References

Aggarwal, S K, and R MacKinnon. 1996. “Contribution of the S4 Segment to Gating Charge in the Shaker K^+ Channel.” *Neuron* 16(6): 1169–77.

Ahern, Christopher a, and Richard Horn. 2004. “Specificity of Charge-Carrying Residues in the Voltage Sensor of Potassium Channels.” *The Journal of General Physiology* 123(March): 205–16.

Akabas, M H, D a Stauffer, M Xu, and a Karlin. 1992. “Acetylcholine Receptor Channel Structure Probed in Cysteine-Substitution Mutants.” *Science (New York, N.Y.)* 258(5080): 307–10.

Bezanilla, Francisco. 2000. “The Voltage Sensor in Voltage-Dependent Ion Channels.” *Physiol Rev.* 80(2): 555–92.

Bezanilla, Francisco, Eduardo Perozo, Diane M Papazian, and Enrico Stefani. 1991. “Molecular Basis of Gating Charge Immobilization in Shaker Gating Charge Potassium Channels.” *Science* 254(5032): 679–83.

Brown, Scott, David P Sonntag, and Michael C Sanguinetti. 2008. “A Highly Conserved Alanine in the S6 Domain of the hERG1 K^+ Channel Is Required for Normal Gating.” *Cell Physiol Biochem.* 22(5-6): 601–10.

Cheng, Yen May et al. 2013. “Functional Interactions of Voltage Sensor Charges with an S2 Hydrophobic Plug in hERG Channels.” *The Journal of general physiology* 142(3): 289–303.

Curran, M E et al. 1995. “A Molecular Basis for Cardiac Arrhythmia: HERG Mutations Cause Long QT Syndrome.” *Cell* 80(5): 795–803.

Dou, Ying et al. 2013. “The Neutral, Hydrophobic Isoleucine at Position I521 in the Extracellular S4 Domain of hERG Contributes to Channel Gating Equilibrium.” *American journal of physiology. Cell physiology* 305(4): C468–78.

Doyle, D. a. Morais Cabral J, Pfuetzner RA, Kuo A, Gulbis JM, Cohen SL, Chait BT, MacKinnon R. 1998. “The Structure of the Potassium Channel: Molecular Basis of K+ Conduction and Selectivity.” *Science* 280(5360): 69–77.

Durdagi, Serdar, Sumukh Deshpande, Henry J Duff, and Sergei Y Noskov. 2012. “Modeling of Open, Closed, and Open-Inactivated States of the hERG1 Channel: Structural Mechanisms of the State-Dependent Drug Binding.” *Journal of chemical information and modeling* 52(10): 2760–74.

Es-Salah-Lamoureux, Zeineb et al. 2010. "Fluorescence-Tracking of Activation Gating in Human ERG Channels Reveals Rapid S4 Movement and Slow Pore Opening." *PloS one* 5(5): e10876.

Fedida, David, and John Christian Hesketh. 2001. "Gating of Voltage-Dependent Potassium Channels." *Prog Biophys Mol Biol.* 75(3): 165–99.

Ferrer, Tania, Jason Rupp, David R Piper, and Martin Tristani-Firouzi. 2006. "The S4-S5 Linker Directly Couples Voltage Sensor Movement to the Activation Gate in the Human Ether-a'-Go-Go-Related Gene (hERG) K+ Channel." *The Journal of Biological Chemistry* 281(18): 12858–64.

Giudicessi, John R, and Michael J Ackerman. 2012. "Potassium-Channel Mutations and Cardiac Arrhythmias--Diagnosis and Therapy." *Nature reviews. Cardiology* 9(6): 319–32.

Gong, Qiuming, Corey L Anderson, Craig T January, and Zhengfeng Zhou. 2004. "Pharmacological Rescue of Trafficking Defective HERG Channels Formed by Coassembly of Wild-Type and Long QT Mutant N470D Subunits." *American Journal of Physiology. Heart and Circulatory Physiology* 287: H652–58.

Goodchild, Samuel J, and David Fedida. 2013. "Gating Charge Movement Precedes Ionic Current Activation in hERG Channels." *Channels (Austin, Tex.)* 8(1): 84–89.

Hardman, Rachael M et al. 2007. "Activation Gating of hERG Potassium Channels: S6 Glycines Are Not Required as Gating Hinges." *The Journal of biological chemistry* 282(44): 31972–81.

Huang, F.-D. et al. 2001. "Long-QT Syndrome-Associated Missense Mutations in the Pore Helix of the HERG Potassium Channel." *Circulation* 104(9): 1071–75.

Islas, L D, and F J Sigworth. 1999. "Voltage Sensitivity and Gating Charge in *Shaker* and *Shab* Family Potassium Channels." *The Journal of General Physiology* 114 (November): 723–42.

Jiang, Youxing et al. 2002. "The Open Pore Conformation of Potassium Channels." *Nature* 417(6888): 523–26.

Jiang, Youxing et al. 2003. "X-Ray Structure of a Voltage-Dependent K^+ Channel." *Nature* 423(6935): 33–41.

Kaplan, W D, and W E Trout. 1969. "The Behavior of Four Neurological Mutants of *Drosophila*." *Genetics* 61(2): 399–409.

Larsson, H P, O S Baker, D S Dhillon, and E Y Isacoff. 1996. "Transmembrane Movement of the *Shaker* K^+ Channel S4." *Neuron* 16(2): 387–97.

Lee, Seok-Yong, Anirban Banerjee, and Roderick MacKinnon. 2009. “Two Separate Interfaces between the Voltage Sensor and Pore Are Required for the Function of Voltage-Dependent K^+ Channels.” *PLoS biology* 7(3): e47.

Lidia M. Mannuzzu, Mario M. Moronne and Ehud Y. Isacoff. 1996. “Direct Physical Measure of Conformational Rearrangement Underlying Potassium Channel Gating.” 271(5246): 213–16.

Lin, Meng-chin, and Diane Papazian. 2007. “Differences Between Ion Binding to Eag and HERG Voltage Sensors Contribute to Differential Regulation of Activation and Deactivation Gating.” *Channels (Austin)* 1(6): 429–37.

Li-smerin, Yingying, David H Hackos, and Kenton J Swartz. 2000. “A-Helical Structural Elements within the Voltage-Sensing Domains of a K^+ Channel.” *J Gen Physiol* 115(January): 33–50.

Liu, Jie, Mei Zhang, Min Jiang, and Gea-Ny Tseng. 2003. “Negative Charges in the Transmembrane Domains of the HERG K Channel Are Involved in the Activation- and Deactivation-Gating Processes.” *The Journal of General Physiology* 121(6): 599–614.

Liu, S et al. 1996. “Activation and Inactivation Kinetics of an E-4031-Sensitive Current from Single Ferret Atrial Myocytes.” *Biophysical journal* 70(June): 2704–15.

Long, Stephen B, Ernest B Campbell, and Roderick Mackinnon. 2005. “Crystal Structure of a Mammalian Voltage-Dependent *Shaker* Family K^+ Channel.” *Science (New York, N.Y.)* 309(5736): 897–903.

Papazian, D M et al. 1995. “Electrostatic Interactions of S4 Voltage Sensor in *Shaker* K^+ Channel.” *Neuron* 14(6): 1293–1301.

Papazian, D M, L C Timpe, Y N Jan, and L Y Jan. 1991. “Alteration of Voltage-Dependence of *Shaker* Potassium Channel by Mutations in the S4 Sequence.” *Nature* 349(6307): 305–10.

Piper, David R et al. 2005. “Regional Specificity of Human Ether-a’-Go-Go-Related Gene Channel Activation and Inactivation Gating.” *The Journal of biological chemistry* 280(8): 7206–17.

Piper, David R et al. 2008. “Cooperative Interactions Between R531 and Acidic Residues in the Voltage Sensing Module of hERG1 Channels.” *Cell Physiol Biochem.* 21(1-3): 37–46.

Piper, David R, Anthony Varghese, Michael C Sanguinetti, and Martin Tristani-Firouzi. 2003. “Gating Currents Associated with Intramembrane Charge Displacement in HERG Potassium Channels.” *Proceedings of the National Academy of Sciences of the United States of America* 100(18): 10534–39.

Pless, Stephan a, Jason D Galpin, Ana P Niciforovic, and Christopher a Ahern. 2011. "Contributions of Counter-Charge in a Potassium Channel Voltage-Sensor Domain." *Nature chemical biology* 7(9): 617–23.

Rocheleau, Jessica M, and William R Kobertz. 2008. "KCNE Peptides Differently Affect Voltage Sensor Equilibrium and Equilibration Rates in KCNQ1 K^+ Channels." *The Journal of General Physiology* 131(1): 59–68.

Sanguinetti, M C, C Jiang, M E Curran, and M T Keating. 1995. "A Mechanistic Link between an Inherited and an Acquired Cardiac Arrhythmia: HERG Encodes the IKr Potassium Channel." *Cell* 81(2): 299–307.

Sanguinetti, M C, and Q P Xu. 1999. "Mutations of the S4-S5 Linker Alter Activation Properties of HERG Potassium Channels Expressed in Xenopus Oocytes." *Journal of Physiology* 514.3: 667–75.

Sanguinetti, Michael C, and Martin Tristani-Firouzi. 2006. "hERG Potassium Channels and Cardiac Arrhythmia." *Nature* 440(7083): 463–69. http://www.ncbi.nlm.nih.gov/pubmed/16554806 (July 21, 2014).

Santacruz-toloza, Lucia, Francisco Bezanilla, and Diane M Papazian. 1994. "S4 Mutations Alter Gating Currents of *Shaker* K^+ Channels." 66(February): 345–54.

Seoh, S a, D Sigg, D M Papazian, and F Bezanilla. 1996. "Voltage-Sensing Residues in the S2 and S4 Segments of the *Shaker* K^+ Channel." *Neuron* 16(6): 1159–67.

Smith, Paula L, and Gary Yellen. 2002. "Fast and Slow Voltage Sensor Movements in HERG Potassium Channels." *J Gen Physiol.* 119(March): 275–93.

Stauffer, D a, and a Karlin. 1994. "Electrostatic Potential of the Acetylcholine Binding Sites in the Nicotinic Receptor Probed by Reactions of Binding-Site Cysteines with Charged Methanethiosulfonates." *Biochemistry* 33(22): 6840–49.

Subbiah, Rajesh N et al. 2004. "Molecular Basis of Slow Activation of the Human Ether- a-Go-Go Related Gene Potassium Channel." *J Physiol.* 558(Pt 2)(Jul): 417–31.

Subbiah, Rajesh N, Mari Kondo, Terence J Campbell, and Jamie I Vandenberg. 2005. "Tryptophan Scanning Mutagenesis of the HERG K^+ Channel: The S4 Domain Is Loosely Packed and Likely to Be Lipid Exposed." 2: 367–79.

Tao, Xiao et al. 2010. "A Gating Charge Transfer Center in Voltage Sensors." *Science (New York, N.Y.)* 328(5974): 67–73.

Thouta, Samrat et al. 2014. "Proline Scan of the HERG Channel S6 Helix Reveals the Location of the Intracellular Pore Gate." *Biophysical journal* 106(5): 1057–69.

Tiwari-woodruff, Seema K, Meng-chin A Lin, Christine T Schulteis, and Diane M Papazian. 2000. "Voltage-Dependent Structural Interactions in the Shaker K Channel." *The Journal of General Physiology* 115(January): 123–38.

Tristani-Firouzi, Martin, Jun Chen, and Michael C. Sanguinetti. 2002. "Interactions between S4-S5 Linker and S6 Transmembrane Domain Modulate Gating of HERG K^+ Channels." *Journal of Biological Chemistry* 277: 18994–0.

Trudeau, M C, J W Warmke, B Ganetzky, and G a Robertson. 1995. "HERG, a Human Inward Rectifier in the Voltage-Gated Potassium Channel Family." *Science (New York, N.Y.)* 269(5220): 92–95.

Vandenberg, J. I. et al. 2012. "hERG K^+ Channels: Structure, Function, and Clinical Significance." *Physiological Reviews* 92(3): 1393–1478.

Wang, S et al. 1997. "A Quantitative Analysis of the Activation and Inactivation Kinetics of HERG Expressed in Xenopus Oocytes." *The Journal of physiology* 502 (Pt 1(1997): 45–60.

Wang, Zhuren et al. 2013. "Components of Gating Charge Movement and S4 Voltage-Sensor Exposure during Activation of hERG Channels." *The Journal of General Physiology* 141(4): 431–43.

Warmke, J W, and B Ganetzky. 1994. "A Family of Potassium Channel Genes Related to Eag in Drosophila and Mammals." *Proceedings of the National Academy of Sciences of the United States of America* 91(8): 3438–42.

Yang, Naibo, Alfred L George, and Richard Horn. 1996. "Molecular Basis of Charge Movement in Voltage-Gated Sodium Channels." *Neuron* 16(1): 113–22.

Yifrach, Ofer, and Roderick Mackinnon. 2002. "Energetics of Pore Opening in a Voltage-Gated K+ Channel." *Cell* 111(2): 231–39.

Zagotta, W N, T Hoshi, J Dittman, and R W Aldrich. 1994. "Shaker Potassium Channel Gating. II: Transitions in the Activation Pathway." *The Journal of General Physiology* 103(2): 279–319.

Zhang, M et al. 2005. "Interactions Between Charged Residues in the Transmembrane Segments of the Voltage-Sensing Domain in the hERG Channel." *J Membr Biol.* 181(207(3)): 169–81.

Zhang, Mei, Jie Liu, and Gea-ny Tseng. 2004. "Gating Charges in the Activation and Inactivation Processes of the hERG Channel." *The Journal of General Physiology* 124(6): 703–718.

Appendices

Appendix A

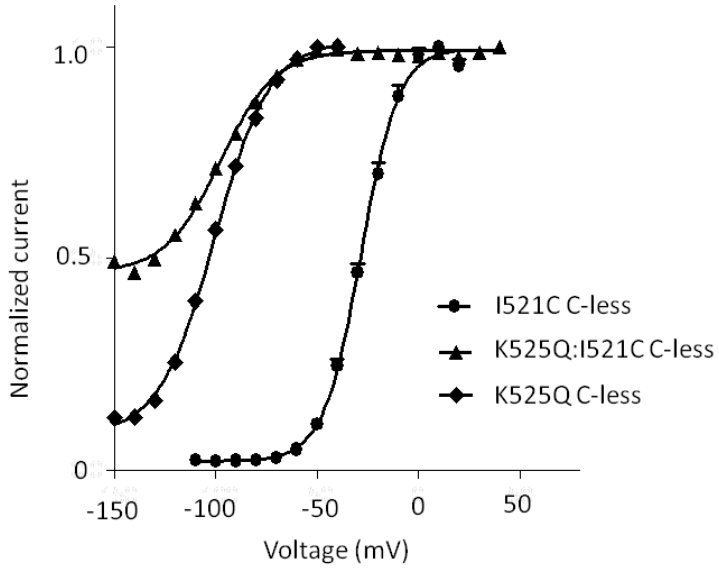

Figure A.1 The G-V relationship for single and double mutant of K525.

To assess the influence of the I521C background, the G-V relationship of a single glutamine-substitution at K525 was measured ($V_{1/2}$ = -100.6 ± 1.2, k = 13.8 ± 1.1).

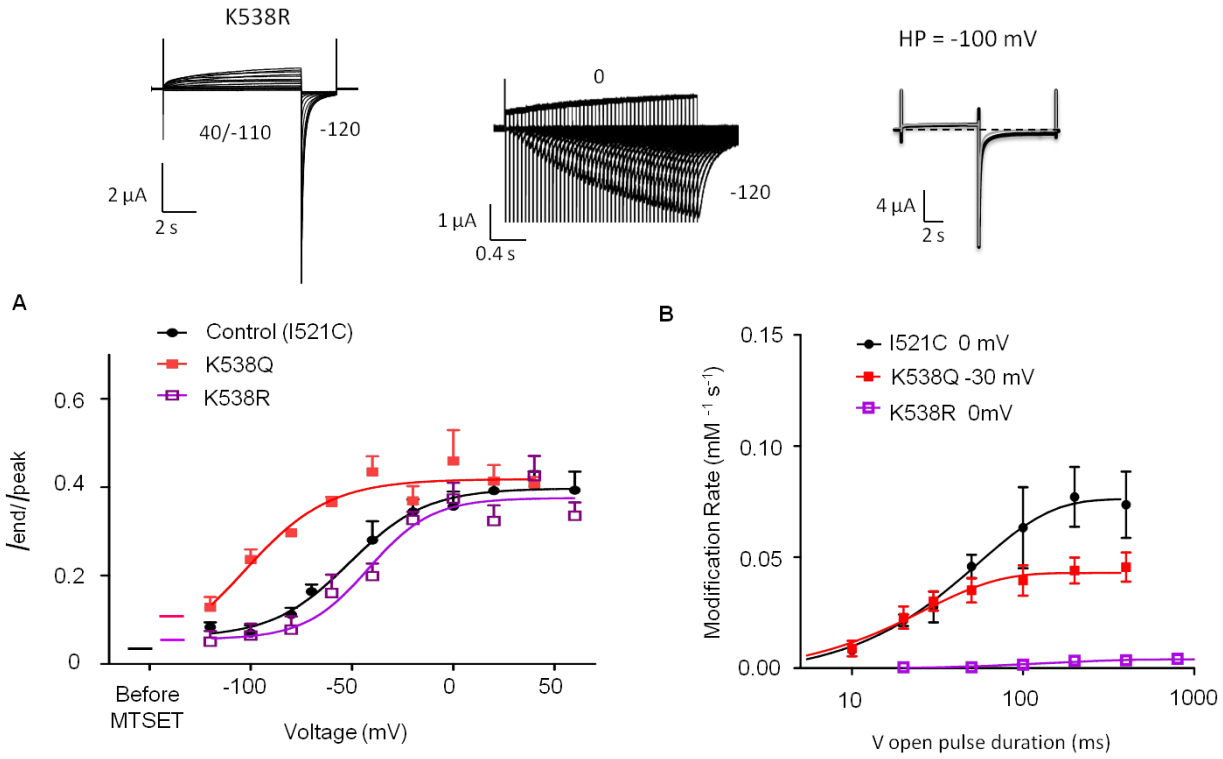

Figure A.2 Summary of testing MTSET modification of the K538R mutant channel.

(A) MTSET modification-voltage relationship for K538 mutations. The K538R activation curve has $V_{1/2}$ = -11.5 ±2.2 mV, k = 7.2 ± 4.2 (n=5) while the MTSET modification-voltage curve has $V_{1/2}$ = -44.4 mV, k = 13.9. (B) The MTSET modification rate for K538R channel. The τ value of channel activation at 0 mV is 1521 ± 154 ms (n=7) while the rate of S4 movement is 145 ms. The proportion of τ of S4 against τ of channel activation is 0.09.

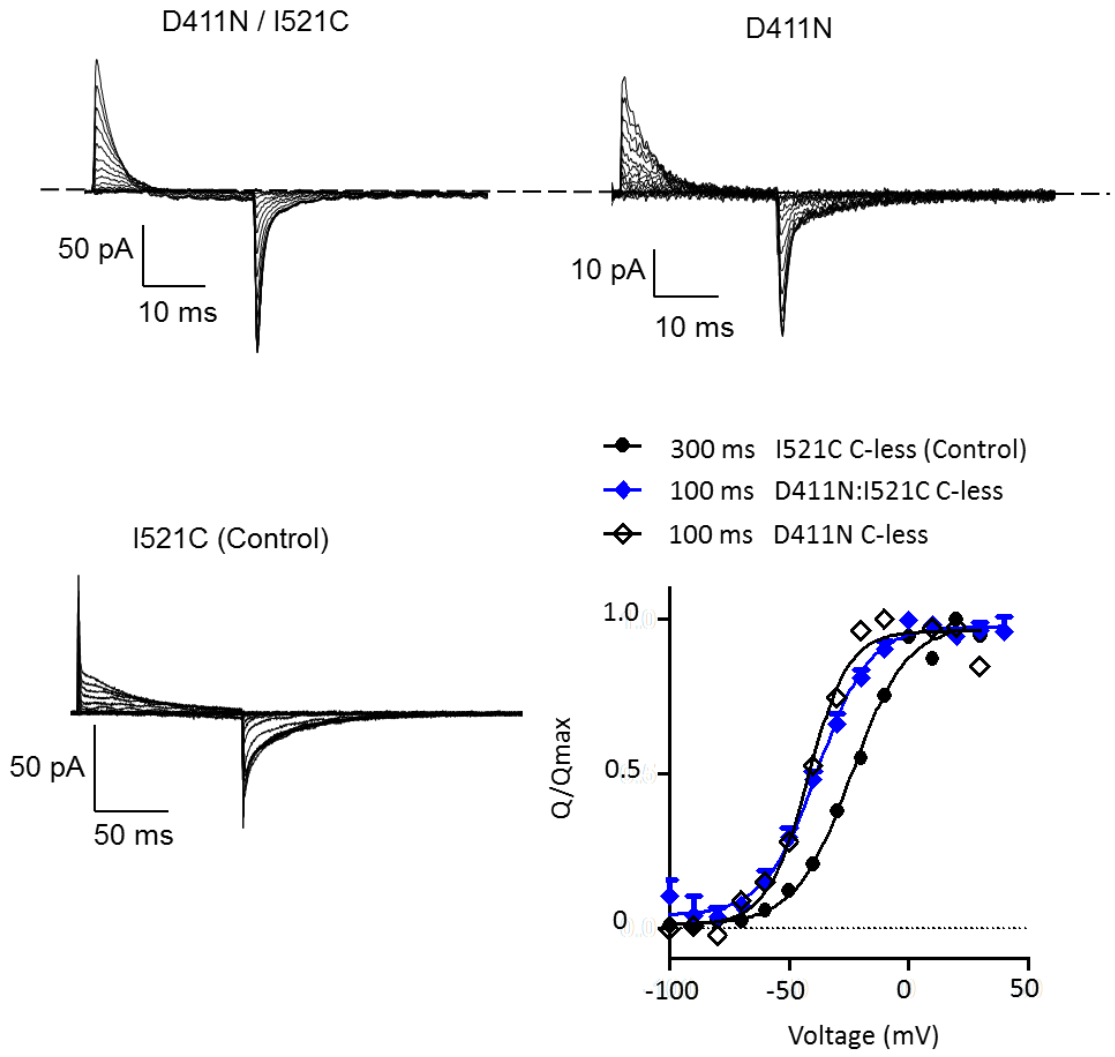

Figure A.3 The influence of I521C background on D411N gating.

Representative gating currents of D411N (right) and D411N within the I521C background (left) evoked by 24 ms depolarizing pulses. Normalized Q_{OFF}-V relationships for control and mutated channels are shown.